ASD TR 61-564

A NEW FORM OF SOLID STATE SOLAR GENERATOR

TECHNICAL REPORT No. ASD TR 61-564

JANUARY 1962

FLIGHT ACCESSORIES LABORATORY
AERONAUTICAL SYSTEMS DIVISION
AIR FORCE SYSTEMS COMMAND
WRIGHT-PATTERSON AIR FORCE BASE, OHIO

PROJECT No. 3145, TASK No. 60959-14

(Prepared under Contract No. AF 33(616)-7637 by
E. D. Fabricius, Giannini Controls Corporation,
Pasadena, California.)

NOTICES

When Government drawings, specifications, or other data are used for any purpose other than in connection with a definitely related Government procurement operation, the United States Government thereby incurs no responsibility nor any obligation whatsoever; and the fact that the Government may have formulated, furnished, or in any way supplied the said drawings, specifications, or other data, is not to be regarded by implication or otherwise as in any manner licensing the holder or any other person or corporation, or conveying any rights or permission to manufacture, use, or sell any patented invention that may in any way be related thereto.

Qualified requesters may obtain copies of this report from the Armed Services Technical Information Agency, (ASTIA), Arlington Hall Station, Arlington 12, Virginia.

This report has been released to the Office of Technical Services, U. S. Department of Commerce, Washington 25, D. C., for sale to the general public.

Copies of ASD Technical Reports and Technical Notes should not be returned to the Aeronautical Systems Division unless return is required by security considerations, contractual obligations, or notice on a specific document.

200 - April 1962 - 26-1098 & 1099

Flight Accessories Laboratory, Aeronautical Systems Division, Wright-Patterson Air Force Base, Ohio.
Rpt No. ASD TR 61-564. A NEW FORM OF SOLID STATE SOLAR GENERATOR. Final rpt, January 1962, 70 p. incl illus & tables.

Unclassified report

This report contains results of an applied research program involving theoretical and experimental investigations directed toward establishing the feasibility of a multiple junction photovoltaic converter. A method of constructing cells having "Tailor Made" voltages is presented. The report covers sample cell fabrication and experimental evaluation and advances a new theory for

(over)

the origin of photoelectrons for the photovoltaic effect in metal - cds photovoltaic junctions.

UNCLASSIFIED

1. Photoelectric cells
2. Photoconductivity
I. AFSC Project 3145
II. Contract AF33(616)-7637
III. Giannini Controls Corp., Pasadena, Calif.
IV. E.D. Fabricius
V. Secondary rpt no. RTR-79
VI. In ASTIA collection
VII. Aval fr OTS

UNCLASSIFIED

Flight Accessories Laboratory, Aeronautical Systems Division, Wright-Patterson Air Force Base, Ohio.
Rpt No. ASD TR 61-564. A NEW FORM OF SOLID STATE SOLAR GENERATOR. Final rpt, January 1962, 70 p. incl illus & tables.

Unclassified report

This report contains results of an applied research program involving theoretical and experimental investigations directed toward establishing the feasibility of a multiple junction photovoltaic converter. A method of constructing cells having "Tailor Made" voltages is presented. The report covers sample cell fabrication and experimental evaluation and advances a new theory for

(over)

the origin of photoelectrons for the photovoltaic effect in metal - cds photovoltaic junctions.

UNCLASSIFIED

1. Photoelectric cells
2. Photoconductivity
I. AFSC Project 3145
II. Contract AF33(616)-7637
III. Giannini Controls Corp., Pasadena, Calif.
IV. E.D. Fabricius
V. Secondary rpt no. RTR-79
VI. In ASTIA collection
VII. Aval fr OTS

UNCLASSIFIED

Flight Accessories Laboratory , Aeronautical Systems Division, Wright-Patterson Air Force Base, Ohio.
Rpt No. ASD TR 61-564. A NEW FORM OF SOLID STATE SOLAR GENERATOR. Final rpt, January 1962, 70 p. incl illus & tables.

Unclassified report

This report contains results of an applied research program involving theoretical and experimental investigations directed toward establishing the feasibility of a multiple junction photovoltaic converter. A method of constructing cells having "Tailor Made" voltages is presented. The report covers sample cell fabrication and experimental evaluation and advances a new theory for

(over)

UNCLASSIFIED

1. Photoelectric cells
2. Photoconductivity
I. AFSC Project 3145
II. Contract AF33(616)-7637
III. Giannini Controls Corp., Pasadena, Calif.
IV. E.D. Fabricius
V. Secondary rpt no. RTR-79
VI. In ASTIA collection
VII. Aval fr OTS

UNCLASSIFIED

Flight Accessories Laboratory , Aeronautical Systems Division, Wright-Patterson Air Force Base, Ohio.
Rpt No. ASD TR 61-564. A NEW FORM OF SOLID STATE SOLAR GENERATOR. Final rpt, January 1962, 70 p. incl illus & tables.

Unclassified report

This report contains results of an applied research program involving theoretical and experimental investigations directed toward establishing the feasibility of a multiple junction photovoltaic converter. A method of constructing cells having "Tailor Made" voltages is presented. The report covers sample cell fabrication and experimental evaluation and advances a new theory for

(over)

UNCLASSIFIED

1. Photoelectric cells
2. Photoconductivity
I. AFSC Project 3145
II. Contract AF33(616)-7637
III. Giannini Controls Corp., Pasadena, Calif.
IV. E.D. Fabricius
V. Secondary rpt no. RTR-79
VI. In ASTIA collection
VII. Aval fr OTS

UNCLASSIFIED

the origin of photoelectrons for the photovoltaic effect in metal - cds photovoltaic junctions.

UNCLASSIFIED

the origin of photoelectrons for the photovoltaic effect in metal - cds photovoltaic junctions.

UNCLASSIFIED

Flight Accessories Laboratory , Aeronautical Systems Division, Wright-Patterson Air Force Base, Ohio.
Rpt No. ASD TR 61-564. A NEW FORM OF SOLID STATE SOLAR GENERATOR. Final rpt, January 1962, 70 p. incl illus & tables.

Unclassified report

This report contains results of an applied research program involving theoretical and experimental investigations directed toward establishing the feasibility of a multiple junction photovoltaic converter. A method of constructing cells having "Tailor Made" voltages is presented. The report covers sample cell fabrication and experimental evaluation and advances a new theory for

(over)

UNCLASSIFIED

1. Photoelectric cells
2. Photoconductivity
I. AFSC Project 3145
II. Contract AF33(616)-7637
III. Giannini Controls Corp., Pasadena, Calif.
IV. E.D. Fabricius
V. Secondary rpt no. RTR-79
VI. In ASTIA collection
VII. Aval fr OTS

UNCLASSIFIED

Flight Accessories Laboratory , Aeronautical Systems Division, Wright-Patterson Air Force Base, Ohio.
Rpt No. ASD TR 61-564. A NEW FORM OF SOLID STATE SOLAR GENERATOR. Final rpt, January 1962, 70 p. incl illus & tables.

Unclassified report

This report contains results of an applied research program involving theoretical and experimental investigations directed toward establishing the feasibility of a multiple junction photovoltaic converter. A method of constructing cells having "Tailor Made" voltages is presented. The report covers sample cell fabrication and experimental evaluation and advances a new theory for

(over)

UNCLASSIFIED

1. Photoelectric cells
2. Photoconductivity
I. AFSC Project 3145
II. Contract AF33(616)-7637
III. Giannini Controls Corp., Pasadena, Calif.
IV. E.D. Fabricius
V. Secondary rpt no. RTR-79
VI. In ASTIA collection
VII. Aval fr OTS

UNCLASSIFIED

the origin of photoelectrons for the photovoltaic effect in metal - cds photovoltaic junctions.

UNCLASSIFIED

the origin of photoelectrons for the photovoltaic effect in metal - cds photovoltaic junctions.

UNCLASSIFIED

Flight Accessories Laboratory, Aeronautical Systems Division, Wright-Patterson Air Force Base, Ohio.
Rpt No. ASD TR 61-564. A NEW FORM OF SOLID STATE SOLAR GENERATOR. Final rpt, January 1962, 70 p. incl illus & tables.

Unclassified report

This report contains results of an applied research program involving theoretical and experimental investigations directed toward establishing the feasibility of a multiple junction photovoltaic converter. A method of constructing cells having "Tailor Made" voltages is presented. The report covers sample cell fabrication and experimental evaluation and advances a new theory for

(over)

UNCLASSIFIED

1. Photoelectric cells
2. Photoconductivity
I. AFSC Project 3145
II. Contract AF33(616)-7637
III. Giannini Controls Corp., Pasadena, Calif.
IV. E.D. Fabricius
V. Secondary rpt no. RTR-79
VI. In ASTIA collection
VII. Aval fr OTS

UNCLASSIFIED

Flight Accessories Laboratory, Aeronautical Systems Division, Wright-Patterson Air Force Base, Ohio.
Rpt No. ASD TR 61-564. A NEW FORM OF SOLID STATE SOLAR GENERATOR. Final rpt, January 1962, 70 p. incl illus & tables.

Unclassified report

This report contains results of an applied research program involving theoretical and experimental investigations directed toward establishing the feasibility of a multiple junction photovoltaic converter. A method of constructing cells having "Tailor Made" voltages is presented. The report covers sample cell fabrication and experimental evaluation and advances a new theory for

(over)

UNCLASSIFIED

1. Photoelectric cells
2. Photoconductivity
I. AFSC Project 3145
II. Contract AF33(616)-7637
III. Giannini Controls Corp., Pasadena, Calif.
IV. E.D. Fabricius
V. Secondary rpt no. RTR-79
VI. In ASTIA collection
VII. Aval fr OTS

UNCLASSIFIED

the origin of photoelectrons for the photovoltai~ effect in metal - cds photovoltaic junctions.

UNCLASSIFIED

the origin of photoelectrons for the photovoltaic effect in metal - cds photovoltaic junctions.

UNCLASSIFIED

ABSTRACT

This is a complete report of the work done in the investigation of variable voltage photovoltaic converters, with the objective of establishing the feasibility and operating characteristics of a proposed "New Form of Solid State Solar Generator."

The investigation done under this contract has been successful in that valuable new information related to the origin of the photoconducting electrons in the photovoltaic effect in CdS has been obtained. This information is pertinent to the design and construction of metal-semiconductor solar cells, in that both the photovoltage and the efficiency of metal-semiconductor cells is dependent upon whether electrons are injected from the metal or excited across the forbidden gap of the semiconductor.

This study included an investigation of the effects of geometry, film thickness of rectifying electrode, and resistivity of CdS upon the photovoltage obtainable. A light resistivity of 300 to 600 ohm-cm at 6.3 mw/cm^2 and an electrode film thickness of 4000 to 5000 Å were found to produce the maximum photovoltage.

The origin of the electrons producing the photocurrent has been determined and a geometry for optimizing the photocurrent is given.

Cells designed by evaporating contacts connected in series are shown to give an additive photovoltage.

Suggestions for improving the efficiency are given in the light of experimental evidence.

While batteries producing nine volts were not successfully constructed due to experimental difficulties, the evidence obtained verifies the feasibility of the basic design.

TABLE OF CONTENTS

LIST OF FIGURES

List of Figures
cont.

LIST OF TABLES

List of Tables
cont.

1.0 INTRODUCTION

In recent years the utilization of the photovoltaic effect to produce solar generators of electricity has received considerable attention.

There are two mechanisms by which a photovoltage can be developed: 1) By the action of light incident on a PN junction in a semiconductor, or 2) By the action of light incident upon a metal-semiconductor junction.

The PN junction photocell utilizes many standard techniques of the transistor field which are easily reproducible and highly controllable. A particular advantage enjoyed by silicon and germanium photocells is the voluminous amount of basic information available on these two materials, which have been more thoroughly studied and are probably better understood than any other semiconductor elements in the periodic table.

In a PN junction photocell the maximum theoretical open-circuit voltage is limited by the width of the forbidden gap of the material used. The high work functions of silicon and germanium make these materials unsuitable for metal-semiconductor photocells. Thus, emphasis has been placed upon such materials as cadmium sulfide which has a suitable work function and bandgap, but for which very little basic information is available.

The work done to date on metal-semiconductor photocells indicates the need for a much better understanding of the basic properties and the behavior of the semiconducting materials employed as well as the basic solid state physics involved in the fabrication of metal-semiconductor photocells in general before any real progress can be achieved in this direction.

Manuscript released by the author October 1961 for publication as an ASD Technical Report.

ASD TR 61-564

2.0 DISCUSSION

2.1 Surface Preparation.

Several etchants with and without a vacuum bakeout were investigated. None of the treatments had a significant effect on the photovoltage. However, a significant increase in photocurrent was obtained by etching the crystals for thirty seconds in a 4% solution of HCl and HNO_3, followed by several rinses in deionized water and baking out at about $125^{\circ}C$ in a vacuum of at least 10^{-4} millimeters of mercury.

The resistivity of the crystals does not change upon etching but was found to drop as much as an order of magnitude on baking. The cause of this has been traced to the out-diffusion of sulfur during baking, leaving behind an increased concentration of sulfur vacancies.

2.2 Investigation of the Effect of Resistivity of CdS and Film Thickness of Rectifying Electrode Upon Photovoltage.

Dots of gold 1 mm in diameter ranging in thickness from 500 to 5,000 Å were evaporated onto crystals of CdS to form rectifying contacts. A 4,000 Å thick film of indium was evaporated onto the back side of the crystals to form the ohmic contact.

The resistivity of the CdS crystals was measured under chopped light of 6.3 mw/cm^2 intensity from a tungsten light source of color temperature $2850^{\circ}K$. All intensity values listed in this report are related to this same source.

Tables 1 through 4 summarize the results of these experiments.

Number of Units Tested	Resistivity (ohm-cm)	Average Open-Circuit Voltage (mv)
6	0.1 - 10	.01
3	80 - 100	82
1	375	80
1	3,000	10

TABLE 1. Accumulative Result of 500 Å Gold Film at 6.3 mw/cm^2

Number of Units Tested	Resistivity (ohm-cm)	Average Open-Circuit Voltage (mv)
4	1 - 10	38
2	70 - 80	35
3	120 - 160	133
2	250 - 350	285
2	500 - 600	101
2	700 - 800	175
2	800 - 1,000	120
5	10,000 - 15,000	83

TABLE 2. Accumulative Results of 1,000 Å Gold Film at 6.3 mw/cm^2

Number of Units Tested	Resistivity (ohm-cm)	Average Open-Circuit Voltage (mv)
9	10 - 20	31
7	30 - 60	28
6	90 - 170	95
9	300 - 360	162
1	500	180
3	1,000	183
4	10,000 - 13,000	107

TABLE 3. Accumulative Results of 4,000 Å Gold Film at 6.3 mw/cm^2

Number of Units Tested	Resistivity (ohm-cm)	Average Open-Circuit Voltage (mv)
12	30 - 60	10.9
16	60 - 100	78.5
5	100 - 300	126
7	600	413
2	2,800	34
6	4,200 - 5,000	67
3	10,000	0
2	50,000	27
1	150,000	0

TABLE 4. Accumulative Results of 5,000 Å Gold Film at 6.3 mw/cm^2

The voltage dependence on resistivity for the 5,000 Å gold films appears more erratic than the results on 4,000 Å films. However, the general trend is the same and the results indicate that 4,000 Å and 5,000 Å gold films give approximately the same photovoltages for the same resistivities, with the optimum resistivity range being between 300 ohm.cm and 1,000 ohm.cm.

2.3 Copper-Evaporated Cells.

A 1,000 Å film of copper was evaporated on two groups of crystals simultaneously. One group of crystals was then baked at 460°C for one minute in an N_2-atmosphere in order to diffuse the copper into the cadmium sulfide. Estimated depth of diffusion was 10 microns. Both groups then had a 4,000 Å film of indium evaporated on the underside for ohmic contact.

The results for these two groups are listed in Table 5. A slight improvement in photvoltage is shown in the diffused case as compared to the undiffused case.

Number of Units Tested	Resistivity (ohm-cm)	Average Open-Circuit Voltage (mv)	
		Diffused	Undiffused
5	100 - 200	8	5
2	500 - 600	12	3
2	800 - 1,000	125	3

TABLE 5. Comparison of Diffused Cu-CdS Cells and Undiffused Cu-CdS Cells

2.4 Metallic Electron Emission Vs. Semiconductor Electronic Excitation.

When a metal is brought into contact with a semiconductor of lower work function, electrons flow into the metal due to the electronic density gradient until a field is built up in the semiconductor to balance the diffusion current. Thus, a high-resistivity "depleted region" is formed, giving rise to a rectifying junction. (Figure 1.)

The width of the depletion region is a function of the impurity density in the semiconductor and may be obtained from Poisson's equation:

$$\nabla^2 V = \frac{q\,n}{\epsilon} \tag{1}$$

where n is the density of ionized donors

ϵ is the dielectric constant of the semiconductor

q is the electronic charge.

Integration of Eq.(1) for a one-dimensional model yields:

$$x = \left[\frac{2\epsilon V}{q\,n}\right]^{1/2} \tag{2}$$

At $V = \phi_m - \chi_s$, $x = d$, therefore:

$$d = \left[2\epsilon\,\frac{(\phi_m - \chi_s)}{q\,n}\right]^{1/2} \tag{3}$$

Whether the electrons come from the metal or the semiconductor, the maximum photovoltage obtainable will be given by the difference in work functions of the metal and semiconductor.

$$V_{max} = \phi_m - \phi_s \tag{4}$$

However, the work function of the semiconductor is a function of the resistivity (ρ) of the semiconductor.

$$\phi_s(\rho) = E_{vac} - E_f(\rho) \tag{5}$$

where E_{vac} is the energy of an electron at a large distance from the semiconductor

E_f is the Fermi level in the semiconductor.

2.4.1 High Resistivity. For high resistivity materials, Maxwell-Boltzmann statistics applies and the number of electrons in the conduction band is given by:

$$n = N_c \exp\left[-q\,\frac{(E_c - E_f)}{k\,T}\right] \tag{6}$$

where $N_c = \left[\frac{2\pi\, m^* k\, T}{h^2}\right]^{3/2} = 4.8 \times 10^{15}\, T^{3/2}$

if the effective mass, m*, is taken as the electronic mass.

At room temperature, $N_c = 2.5 \times 10^{19}\ cm^{-3}$.

Solving Eq. (6) for E_f: one obtains

$$E_f = E_c + \frac{kT}{q} \ln\left(\frac{n}{N_c}\right) \tag{7}$$

The resistivity of a semiconductor having only one mobile carrier is defined as:

$$\rho \triangleq \frac{1}{q\mu n} \tag{8}$$

where μ is the mobility of the charge carrier.

Taking the electron mobility of cadmium sulfide as 200 cm^2/v sec. (Ref. 1), one obtains:

$$n = \frac{1}{q\mu\rho} = \frac{1}{3.2 \times 10^{-17}\rho} \quad \text{and}$$

$$E_f = E_c - 0.026 \ln (800\rho) = E_c - 0.174 - 0.026 \ln\rho \tag{9}$$

where E is in ev, and ρ is in ohm-cm.

The electron affinity of a semiconductor is defined as:

$$\chi_s \triangleq E_{vac} - E_c \tag{10}$$

Therefore, $\phi_s = \chi_s + 0.174 + 0.026 \ln\rho$, and (11)

$$V_{max} = \phi_m - \chi_s - 0.174 - 0.26 \ln\rho \tag{12}$$

A best fit of three curves for chlorine-doped cadmium sulfide with gold films of different thicknesses yields the following values for contact potential ($\phi_m - \chi_s$), and photovoltage:

Gold Thickness (Å)	Contact Potential (ev)	Photovoltage (v)
500	0.41	$0.230 - 0.026 \ln\rho$
1,000	0.49	$0.310 - 0.026 \ln\rho$
4,000 - 5,000	0.54	$0.358 - 0.026 \ln\rho$

TABLE 6. Contact Potential and Photovoltage of Cadmium Sulfide as a Function of Resistivity for Various Film Thicknesses of Gold

A graph of the above three curves and the experimentally obtained points is shown in Figure 2. As seen from Figure 2, Eq. (12) is a good approximation for resistivities above the peak values in the curves.

2.4.2 Low Resistivity. Substitution of Eq. (8) into Eq. (3) gives the width of the depletion region as a function of resistivity.

$$d = \left[\frac{2\epsilon\mu(\phi_m - \chi_s)}{q}\right]^{1/2} = 1.88 \times 10^{-5} \rho^{1/2} \qquad (13)$$

Thus, if electrons are excited across the forbidden gap, the decrease in d with decreasing resistivity will cause the cross-section for photon capture in the depletion region to drop, resulting in a drop in photovoltage. If, on the other hand, the electrons are coming from the metal, decreasing d will increase the probability of quantum mechanical tunneling at a lower value than V_{max}, again decreasing the photovoltage.

However, quantum mechanical tunneling is not important above 0.1 ohm-cm and cannot therefore be responsible for the observed voltage decrease at low resistivity.

When light enters a solid its intensity decreases exponentially with penetration distance x.

$$I = I_0 \exp\left(\frac{-4\pi\alpha x}{\lambda_0}\right) \qquad (14)$$

where λ_0 is the vacuum wavelength of the light and α is the absorption index.

For light of wavelength 5,000 Å, the absorption index of gold is 1.5 (Ref.2). A calculation of Eq. (14) for various film thicknesses of gold is shown in Table 7.

Gold Thickness angstroms	Transmitted Light I/I_0,%	Absorbed Light, L %
500	15	85
1,000	2.25	98
3,000	1.6×10^{-3}	100
4,000	2.7×10^{-5}	100
5,000	6×10^{-7}	100

TABLE 7. Light Absorption as a Function of Thickness for Gold

Thus, even though electrons 1,000 Å from the surface of a metal may be excited by incident radiation and escape from the surface of the metal (Ref.3), a film thickness of 4,000 Å of gold will absorb all the incident light without ejecting electrons into the cadmium sulfide. Therefore, the electrons must be primarily coming from the cadmium sulfide around the periphery of the gold dot. Shadowing around the edges of the gold dots is quite likely, since the crystals are too thin and brittle to clamp the mask over them during evaporation. This would allow some of the normal light to see a thinner film of gold around the periphery and eject electrons from this region.

2.4.3 Experimental Procedure. To determine the origin of the photo-conducting electrons crystals were mounted on a motor-driven compound slide rest. A 3 x 7 mil^2 slit of light of about 14 mw/cm^2 intensity was focused through a microscope upon the crystal. The current output of the crystal was amplified by a Hewlett-Packard D-C Microammeter and read on a Brown Recording Potentiometer.

The first cell tested (5,000 Å Au), showed no current until the light beam touched the gold. At this point the current rose rapidly to a peak which occurred when the light beam was centered on the edge of the gold dot. The current had again dropped to zero when the light beam was completely on the gold stripe. The current remained zero until the light beam again started off the gold stripe on the opposite edge. The effect is reproducible with the current density varying by a factor of two. The second peak, however, was found to be larger than the first peak by a factor of from 3 to 5 every time. (See Figure 3., -3a). It was thought that this was due to electrons being excited in the barrier region and moving to the other side of the gold stripe. To check this, the direction of the light beam was reversed and the two peaks were found to reverse their relative intensity. (See Figure 3., -3b).

Figure 4 shows the current of both stripes magnified sufficiently to show the leakage current along the CdS between the stripes.

This crystal was covered with indium on the back side and no current could be read through the crystal, due to back-illumination.

The remainder of the crystals were fabricated with indium around the

back-periphery and mounted on glass slides that were etched in the center to expose the CdS crystal, so that the light could be focused on the junction from both sides of the crystal.

Another cell was constructed also having 5,000 Å of gold film on the CdS. Figure 5 shows the current distribution when light is shining on the front side and on the back side of the crystal. Figure 6 is a magnified graph of the current from the back side of the crystal. The two shoulders on the peak are due to scattering of light entering the crystal and to diffusion of electrons excited within a diffusion length of the junction.

Figure 7 shows the current distribution from the front and back sides of a CdS crystal with 500 Å of gold. This thickness of gold will transmit 15% of the light at a wavelength of 5,000 Å and approximately 60% of the total incident light, thus there is a current from light shining on top of the gold stripe.

Figure 8 shows the current distribution from the front and back sides of a CdS crystal with 1,000 Å of gold after it had been baked in a neutral atmosphere for 30 minutes at a temperature of 380°C. Prior to bakeout the current distribution was identical to that of the crystal with 5,000 Å Au (Figure 5) and is shown in Figure 9.

It was hoped that baking would cause a gold diffusion that would form a p-n junction in the CdS. However, the diffusion appears to have formed a resistivity region in the vicinity of the gold stripe. The current from both sides of the crystal goes to zero at the stripe edges and peaks about 0.005 inches from the stripe edge. The junction has been almost destroyed and the current has gone down by 3 orders of magnitude. The spectral response of this crystal was taken from both sides of the crystal prior to bakeout. The results are shown in Figure 10. After bakeout the current was too low to be read on the spectrometer.

For additional confirmation, gold was evaporated upon another crystal in such a manner that the edge of the gold feathered from 5,000 Å thick to zero thickness. The gold stripe was evaporated in such a manner that the feathered

edge was very narrow at one end of the crystal and was about 15 mils wide at the other end of the crystal.

Figure 11 shows the current distribution across the edge of the gold stripe at 4 different positions from the edge having maximum feathering to the edge having minimum feathering.

Figure 12 shows the current distribution due to light shining through the crystal from the back.

The above data show that the active area of the junction is limited to the periphery of the gold dot, and that the junction cross-section is as indicated in Figure 13. Therefore, the active junction area is given by Eq. (15).

$$\text{Area} = pd \tag{15}$$

where p is the perimeter of the gold stripe

and d is the width of the depletion region.

2.4.4 Drop in V_{max} at Low Resistivity. At low resistivities it is found empirically that a curve of the form

$$V = C\rho^{1/2} = Ad \tag{16}$$

where C and A are constants, fits the data nicely. See Figure 14.

Upon evaluating the constants of proportionality in Eq. (16), it is found that:

$$A = 4.4 \times 10^5 \text{ v/cm} \tag{17}$$

The maximum electric field in the depletion region is

$$E_{max} = \nabla V(\rho)_{x=0} \tag{18}$$

The empirically determined value of A is of the same order of magnitude as E_{max} at low resistivity and could be indicative of an avalanche-type breakdown. Thus, it seems quite reasonable to assume that fields of the order of 4×10^5 v/cm are the limiting fields, in which case the empirically determined lower limit of Eq. (16) is the true lower limit.

Figure 15 is a graph showing the entire resistivity range of interest for 4,000 Å and 5,000 Å gold films.

2.5 Front-Junction Illumination Vs. Back-Junction Illumination. In view of the fact that no current is coming from the light shining on the metallic stripe, it appears likely that a back-lighted cell would have a higher current output than a front-lighted cell. The only detrimental effect this arrangement could have on the photovoltage is to lower it slightly due to absorption of strong radiation away from the junction, thus causing the resistivity of the CdS at the junction to be higher.

To investigate this, several crystals were divided into three groups. 5,000 Å films of copper were evaporated on the back sides of group A, 5,000 Å films of gold were evaporated on the back sides of group B, and 5,000 Å films of gold were evaporated on the front sides of group C as a control group. In each case 4,000 Å films of indium served as the ohmic contact.

The data from groups A, B, and C are shown in Table 8.

It appears that the voltage and current both tend to increase in going from group A to group C. More data are needed to determine whether or not this is a statistical fluctuation, as the results are not definite enough to be conclusive.

Rectifying Contact Material	Units Tested Number	Resistivity ohm.cm	Average Open-Circuit Voltage mv	Average Short-Circuit Current m/a
Group A	1	30 - 60	10	10
Copper,	3	60 - 100	3.7	18
Back Side	7	100 - 300	1.9	10.1
Group B	3	30 - 60	1.2	27
Gold,	5	60 - 100	22	49
Back Side	2	100 - 300	7	2,000
Group C	4	30 - 60	4.6	80
Gold, Front	5	60 - 100	93	137
Side	1	100 - 300	2	26

TABLE 8. Comparison of Accumulative Results

2.6 Surface States.

When surface states are present, a surface barrier is formed in a semiconductor before contact is made to a metal. Large surface state density can play the major role in charge exchange with the metal so that there is little change in the semiconductor depletion region upon contact to metal. Also, high surface state density results in strong surface recombination which tends to trap the free electrons in the vicinity of the metal-semiconductor junction. This in turn would decrease the photovoltage observed, since the electrons being trapped are those seeing the highest potential.

The sensitivity of photovoltage to bulk resistivity of the cadmium sulfide cells indicates that in the crystals used, surface states are not sufficiently dense to overshadow bulk properties. However, a slow increase in photovoltage with time is often observed. This effect is indicative of a filling of slow surface states, and has been observed by other workers in this field (Ref. 4). Degradation of photovoltage due to oxygen and other P-type impurities is also reported in the literature (Refs. 5 and 6).

3.0 FABRICATION OF BATTERIES

Following the preliminary investigations, batteries of several cells in series were constructed by evaporating stripes of gold 0.040 inches wide separated by 0.080 inches on the front side and 0.040 inch stripes of indium under the gold on the back side. See Figure 16.

Data on the three batteries submitted with this report are included in Appendix A.

Attempts to fabricate smaller cells were unsuccessful.

4.0 CONCLUSIONS.

1. In view of the data obtained, a cell having a front junction of maximum periphery would yield the highest efficiency. Figure 17 shows a possible geometrical design to achieve this. This design feature could not have been provided without the knowledge acquired in the present study.

Under the limitations of present vacuum deposition techniques, stripes shaped as shown in Figure 17 can be made as small as 1 mil in width with 0.5 mil separation between stripes. Stripes of this size would allow the effective area of the batteries to be raised to about 25% of the total area and net efficiencies of over 1% can be attained. While this is still lower than the efficiency of conventional CdS solar cells, the design permits a tailor-made output voltage limited only by the maximum number of cells that can be deposited on a crystal. Thus, this type of battery would find application whenever voltages of the order of 10 volts are required at a low current level.

2. These cells exhibit high series resistance. A shallow diffused layer of n^+ material introduced prior to evaporating the ohmic contact should reduce the contact resistance between the metal and cadmium sulfide and therefore increase the efficiency of the cell. Long heat treatments lower the carrier lifetime and thereby also lower the efficiency of a solar cell. Thus, the diffusion time should be as short as practical.

3. No attempt was made to reduce reflection on the metal surface. Surface coating with a material having an index of refraction between that of air and cadmium sulfide would decrease surface reflection and approximately double the efficiency.

4. The cells are found to add in series. This is understandable in the light of the experimental determination of the shape of the depletion region and the source of the current.

The proposed nine volt batteries were not successfully constructed. However, the feasibility of the basic design has been verified.

In examining the tables one will notice slight discrepancies in values of current and voltage. These cells are slightly sensitive to past history.

It has been found that a minimum time of two days in the dark is required to allow these cells to reach full recovery. After exposure to light the current and voltage drops about twenty percent almost instantaneously. The measurements were made after a quasi-steady-state condition had been reached. In this condition the reproducibility of cell measurements is still susceptible to fluctuations of about five percent.

REFERENCES

1. Bube, R. H., Photoconductivity of Solids, p. 269 (John Wiley & Sons, New York, 1960)
2. Gilleo, M. A. "Photoemission From Ag Into Ag Cl, K Br, Na Cl, and New Bands of Photosensitivity in Ag Cl". Phys. Rev., 91, 534 (1953)
3. Thomas, H., "The Outer Photoelectric Effect of the Alkali Metals". Part I. "The Dependence on Layer Thickness for K of the Range of Photoelectron in the Metal". Z. Physik 147, 395, (1957)
4. Lempicki, A., "Anamolous Photovoltaic Effect in ZnS single Crystals". Physics Rev., 113, 1204 (1959
5. WADC Tech. Report 57-770, 108 (1957) "A CdS Solar Generator".
6. WADC Tech. Report 59-340, 62 (1959) "Research on Crystal Growth of CdS".

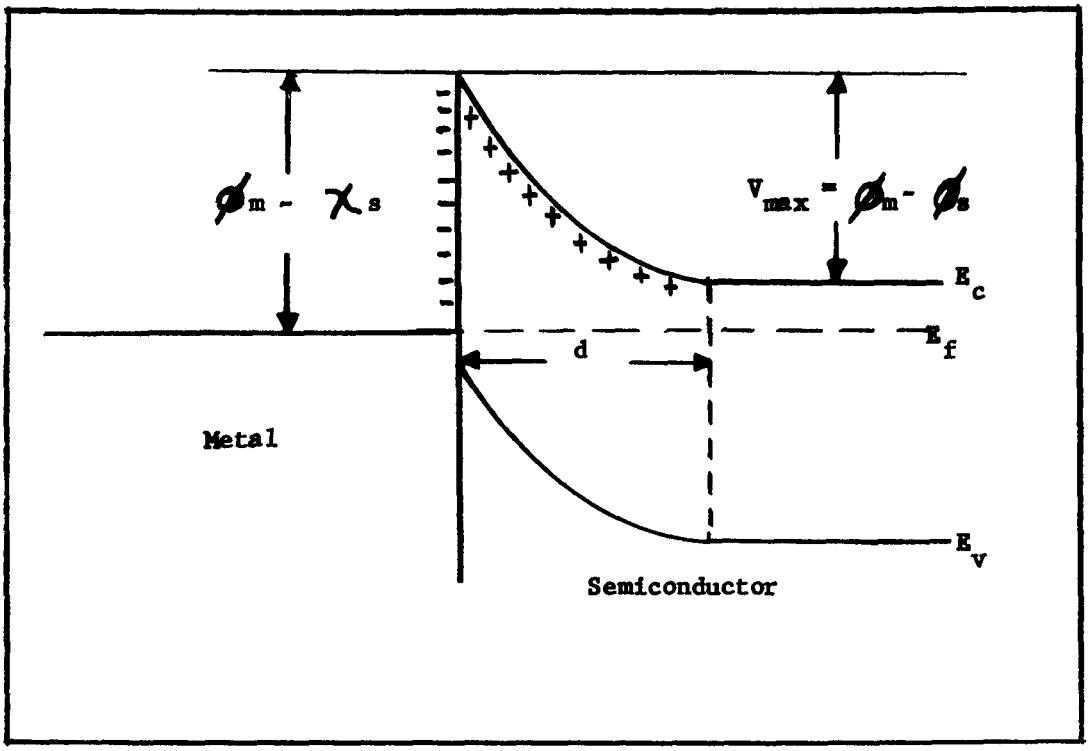

Figure 1. Energy Level Diagram of a Metal-Semiconductor Junction Forming a Rectifying Barrier

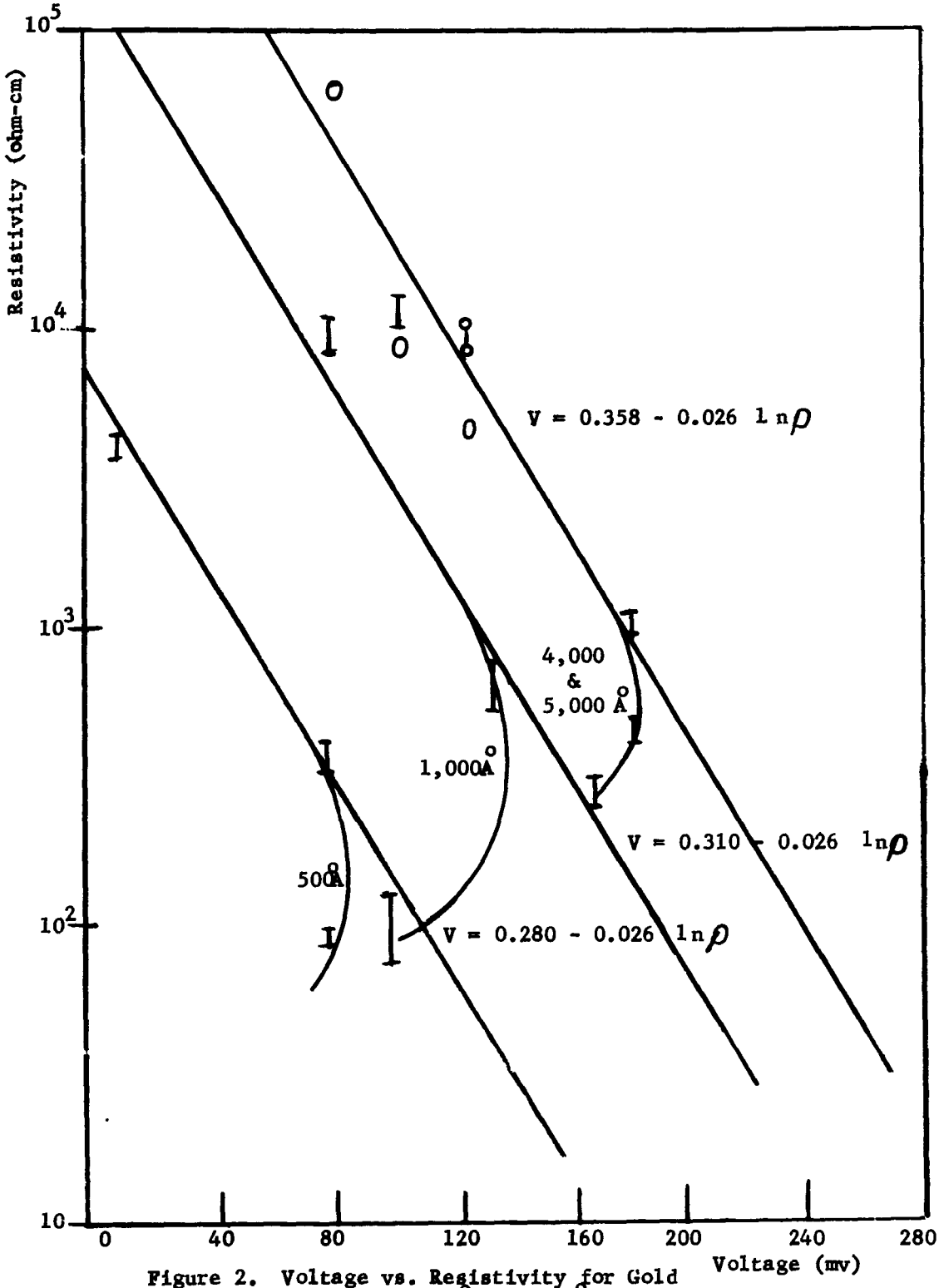

Figure 2. Voltage vs. Resistivity for Gold Films of 500 Å, 1,000 Å, and 4,000 - 5,000 Å at High Resistivities

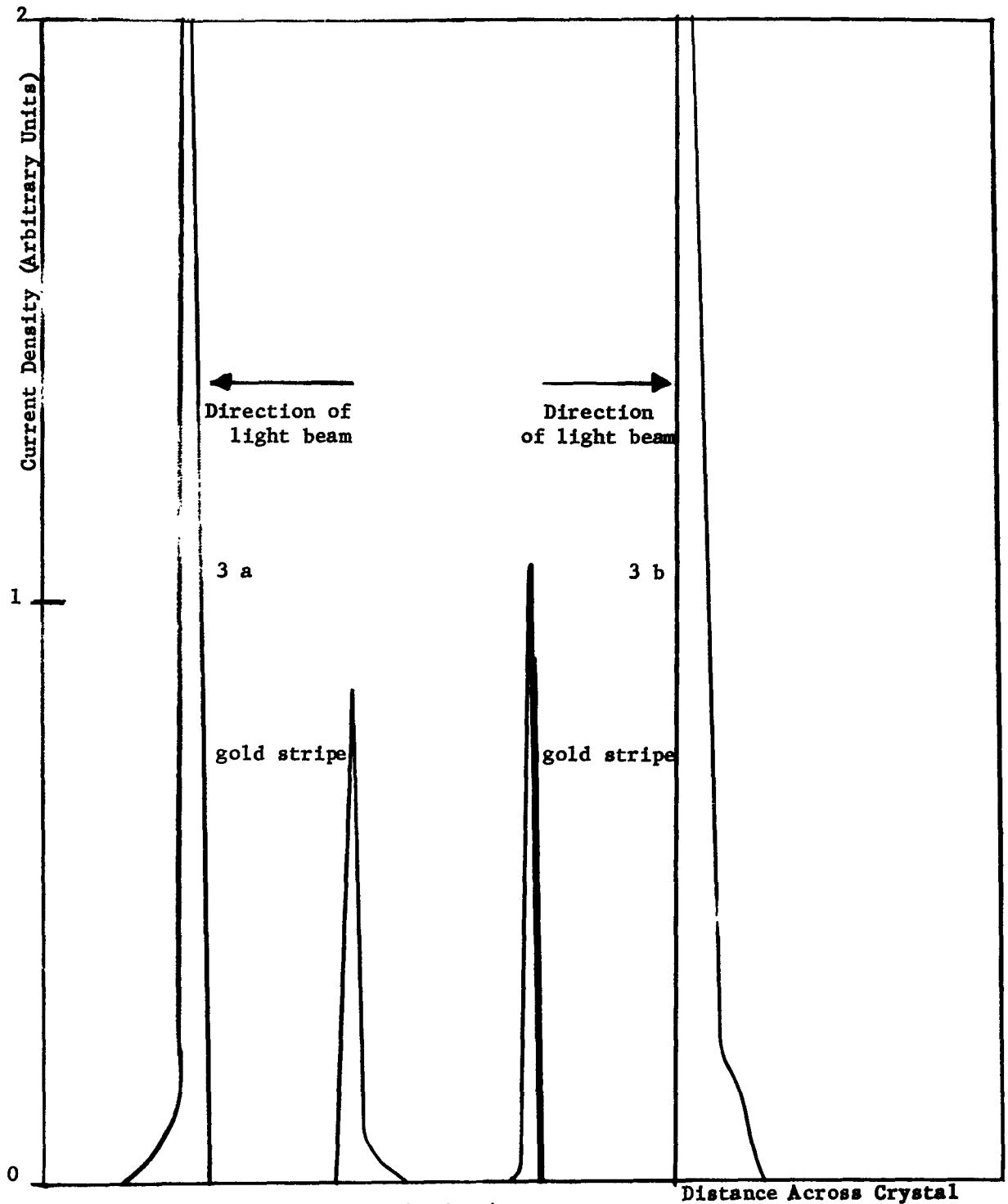

Figure 3. Current Distribution Across Crystal, Showing Effect of Leakage Current

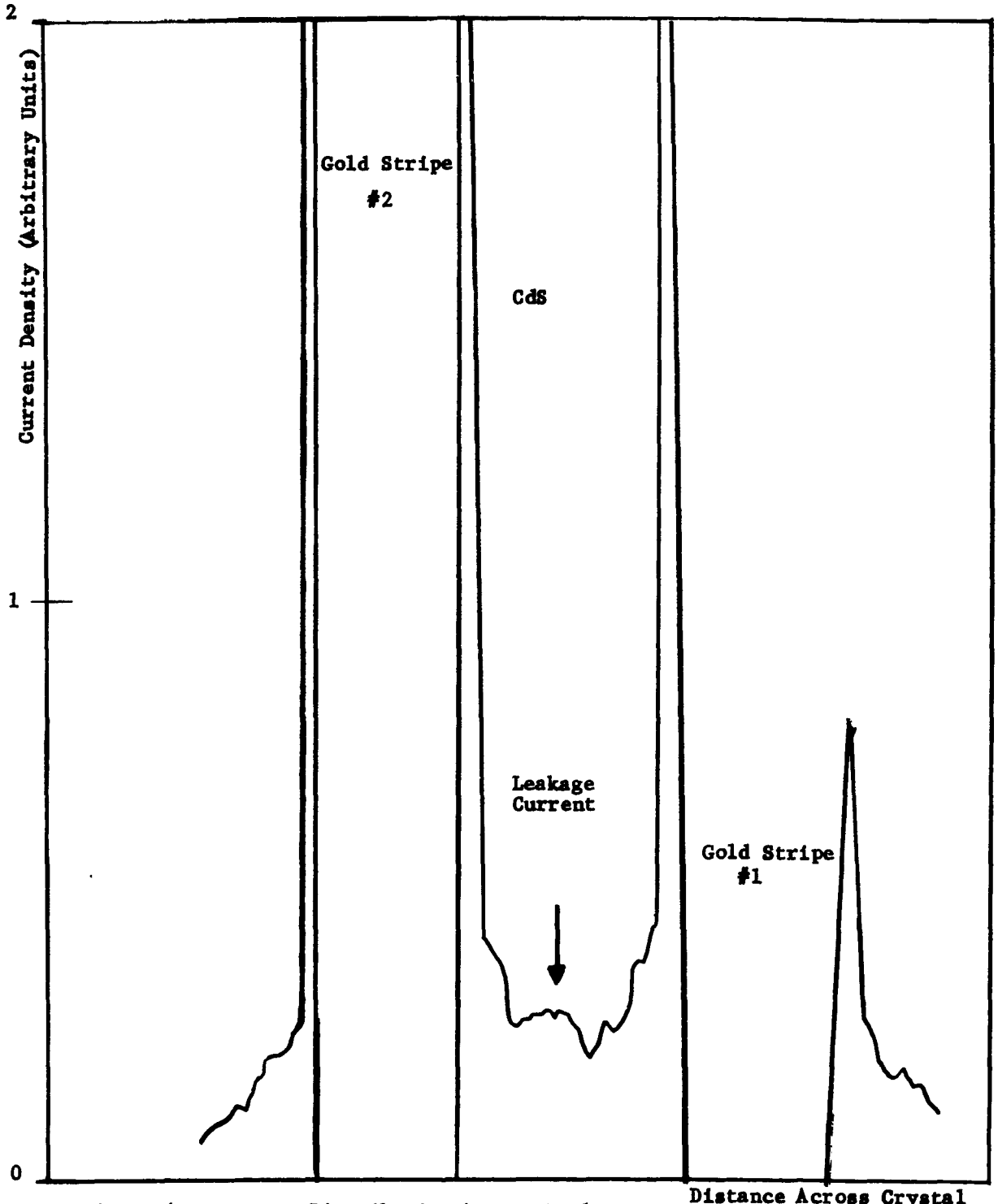

Figure 4. Current Distribution Across Both Stripes of Crystal, Showing Leakage Current Between Gold Stripes

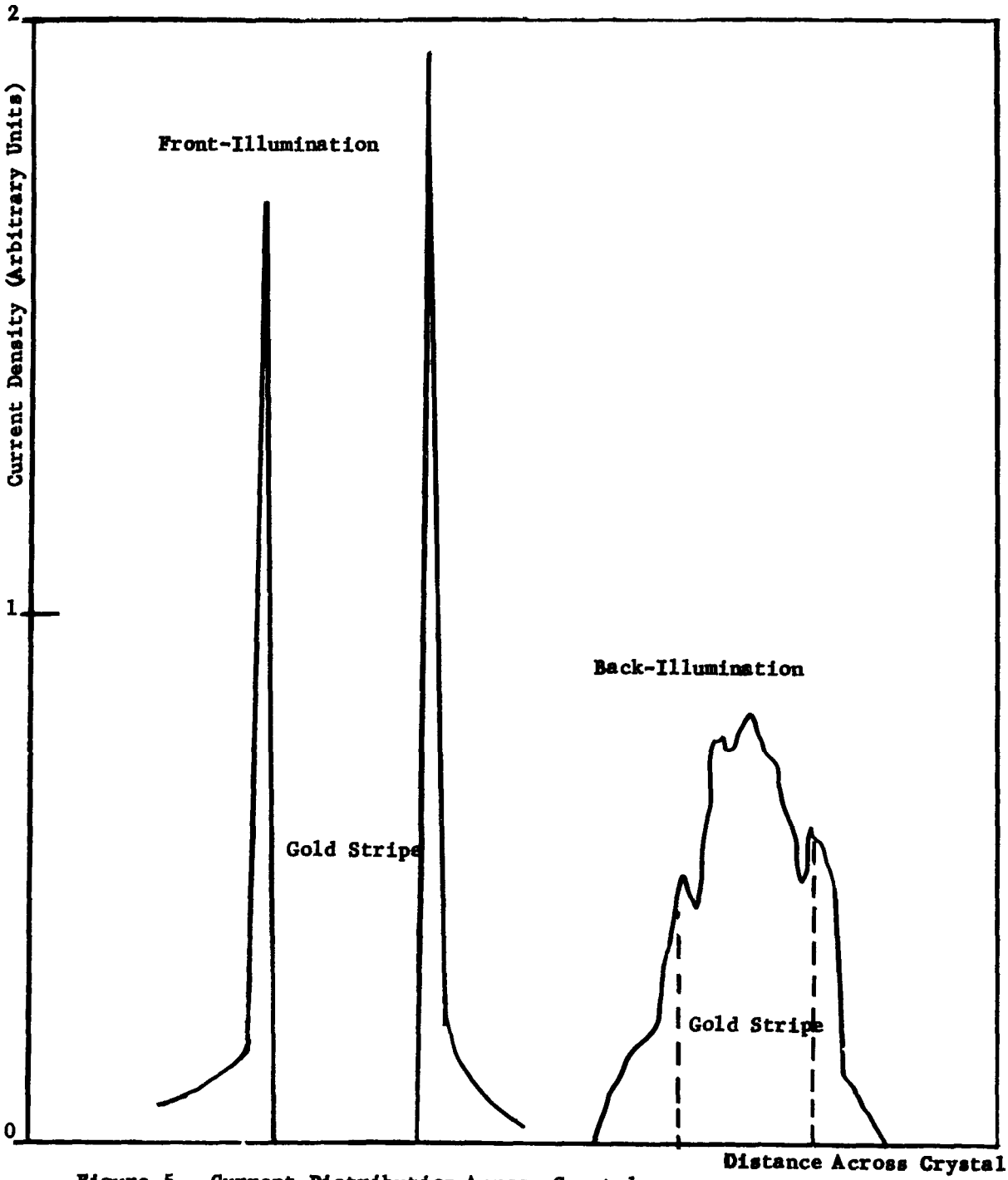

Figure 5. Current Distribution Across Crystal Having a 5,000 Å Au Film

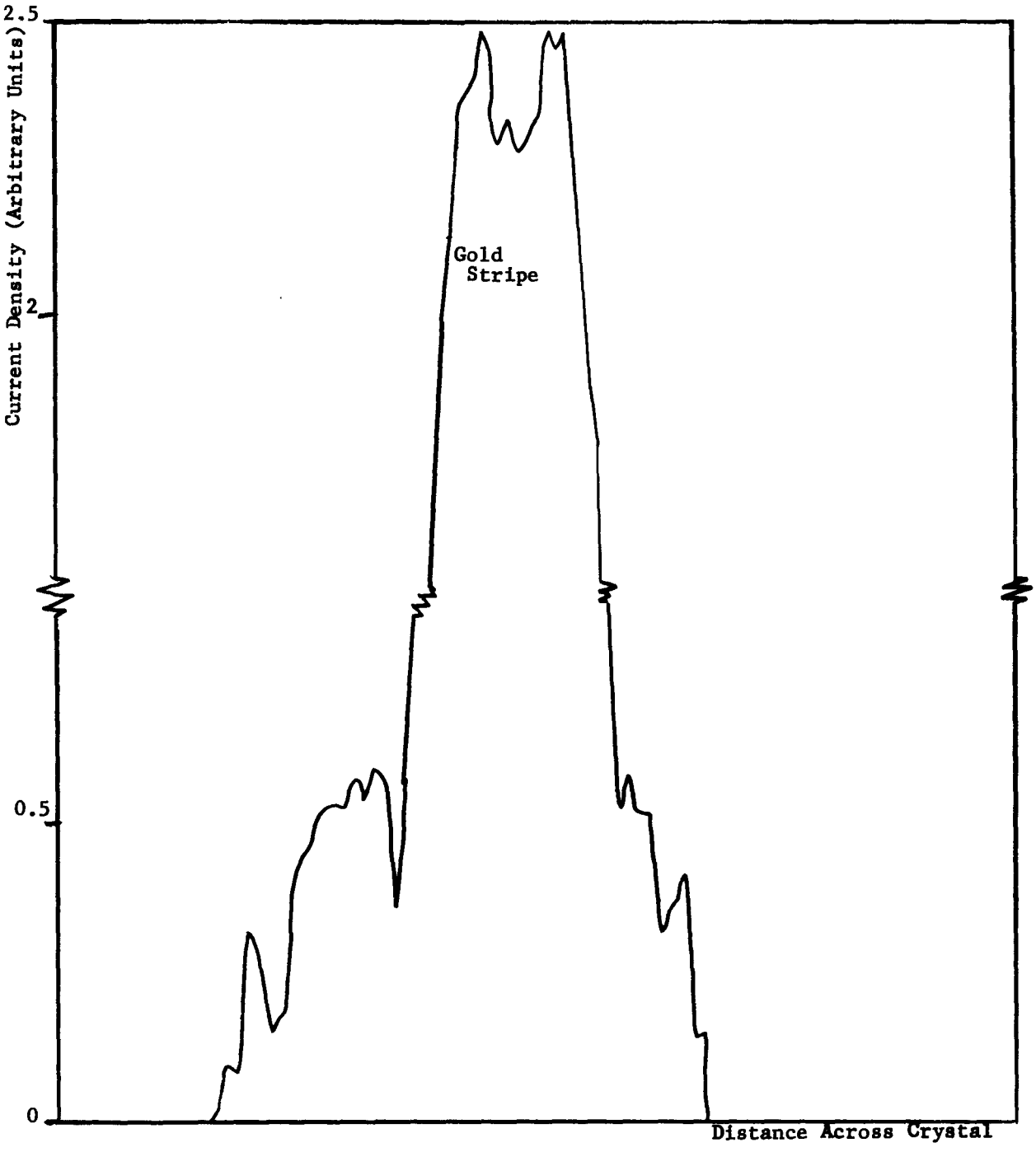

Figure 6. Current Distribution Across Crystal Having a 5,000 Å Au Film, Back-Illumination

(Scale x 3 relative to Figure 3.)

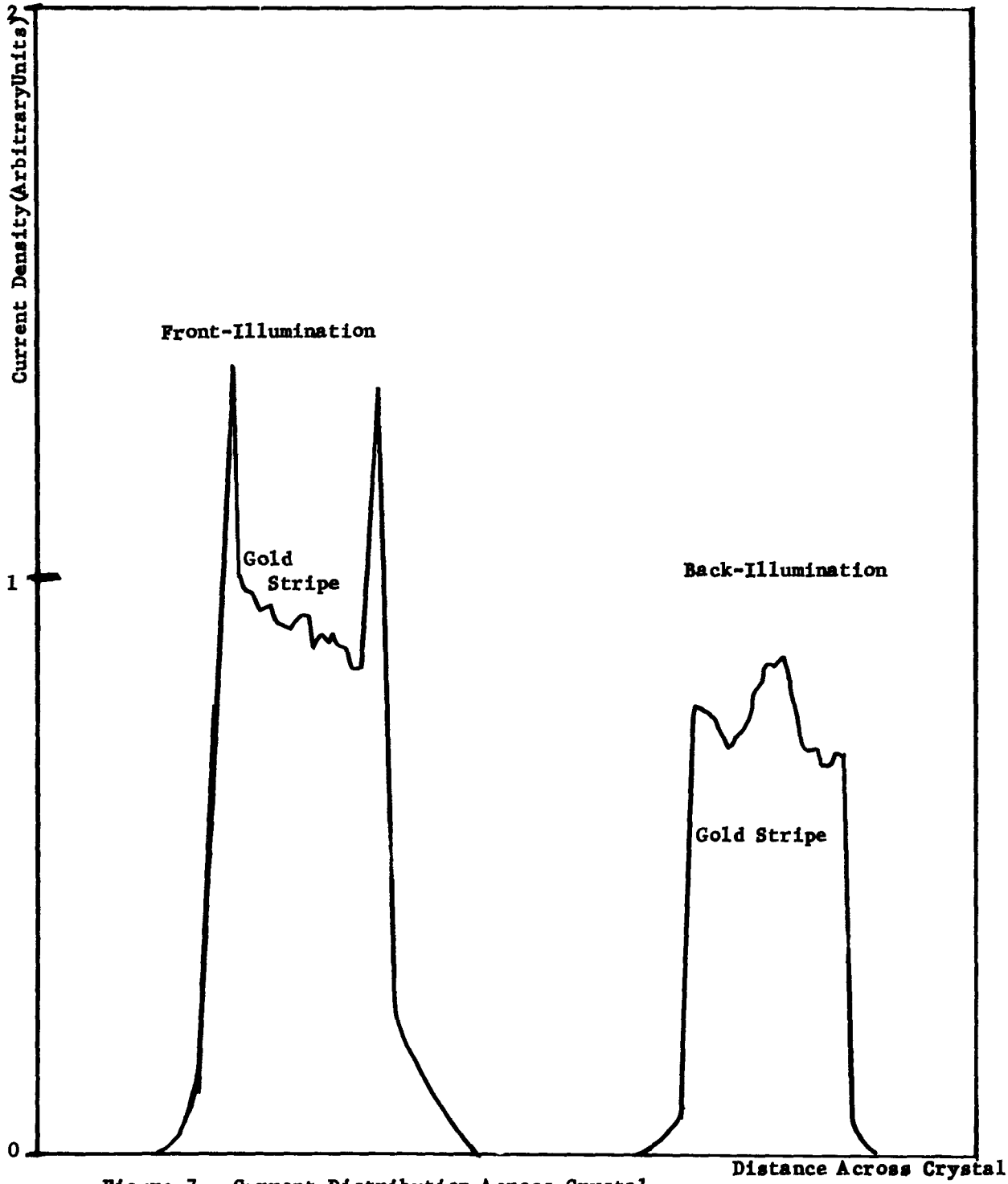

Figure 7. Current Distribution Across Crystal Having a 500 Å Au Film

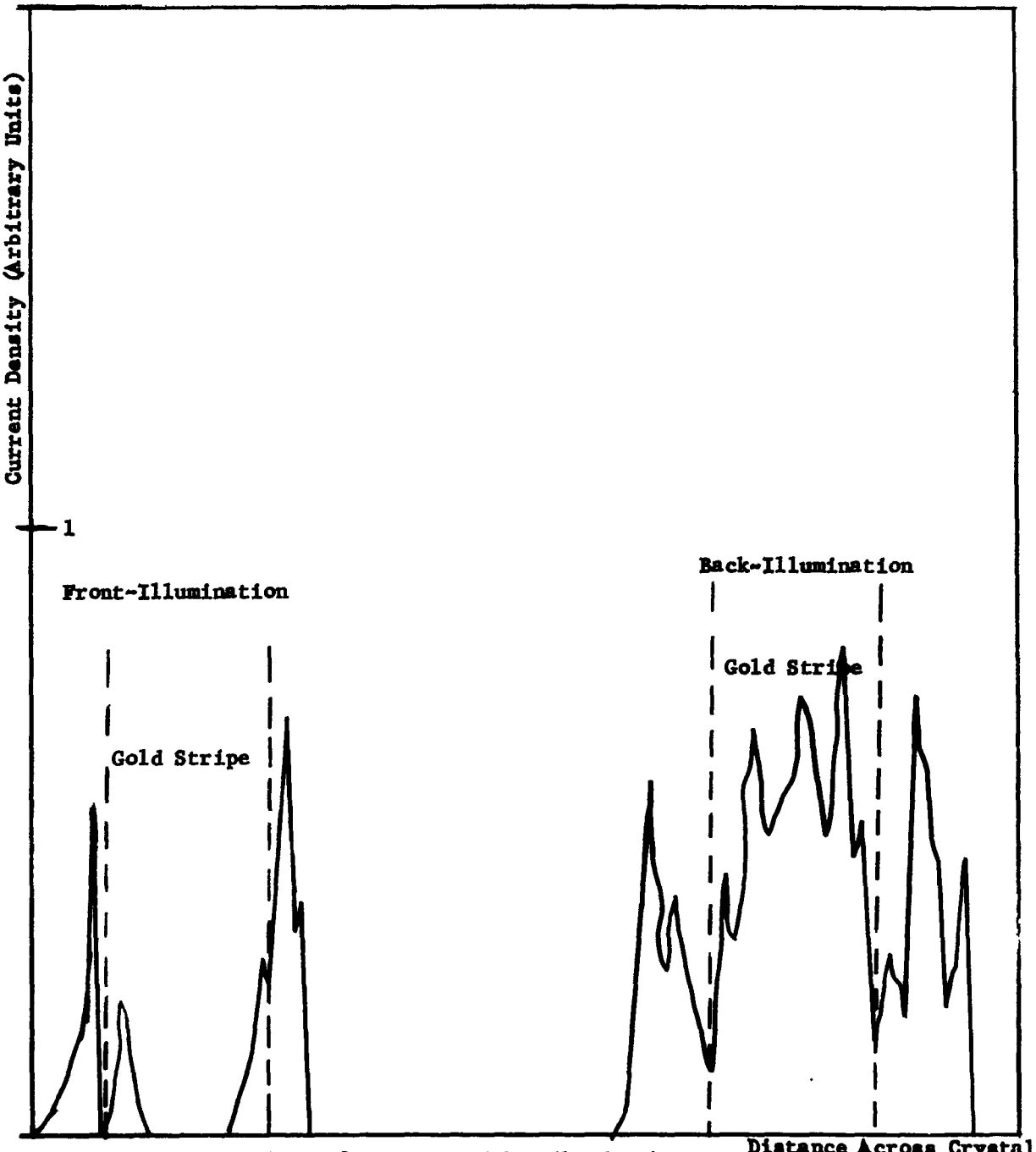

Figure 8. Current Distribution Across Crystal After Bakeout

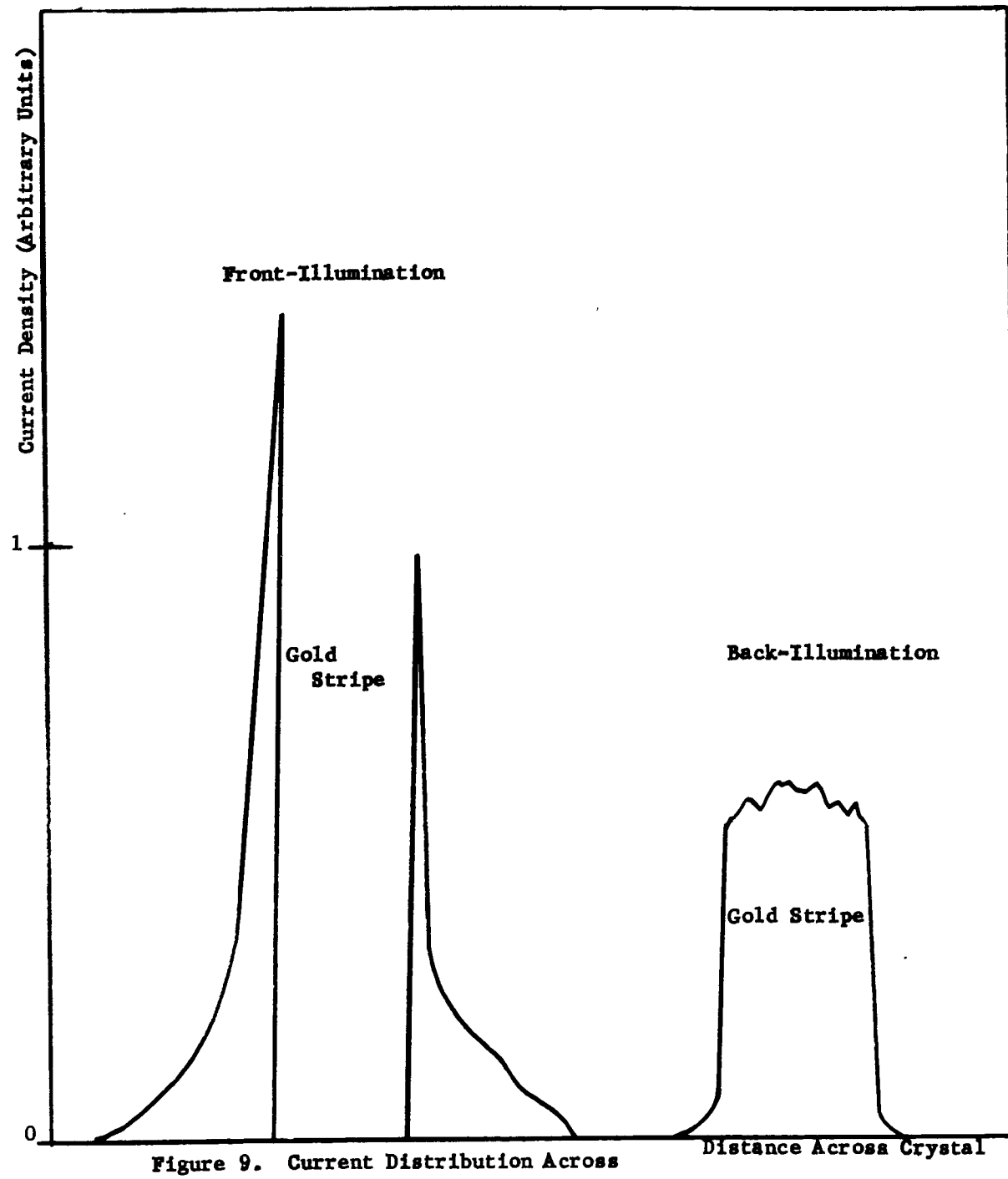

Figure 9. Current Distribution Across Crystal Prior to Bakeout

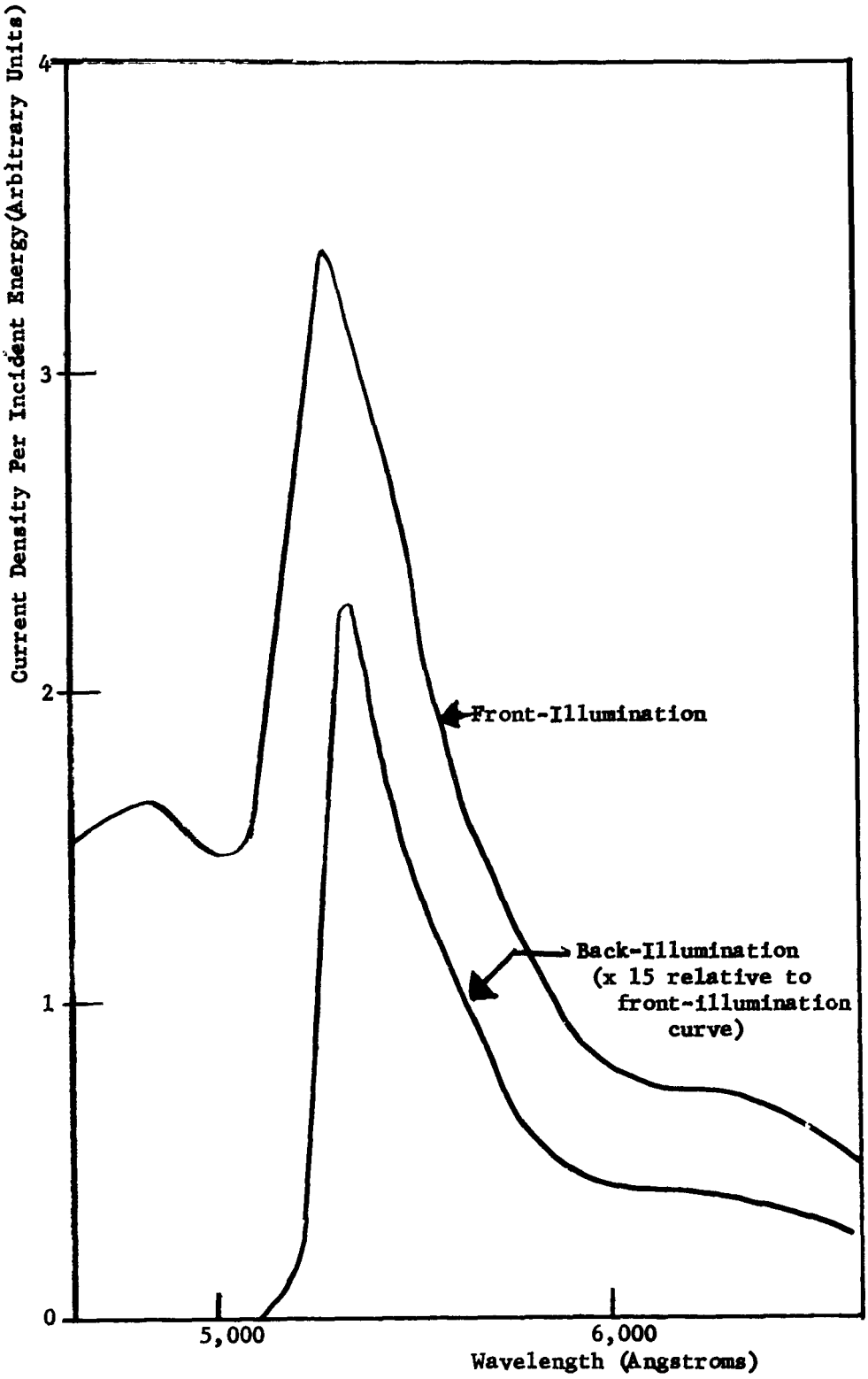

Figure 10. Spectral Response of Au-CdS Crystal due to Front and Back Illumination

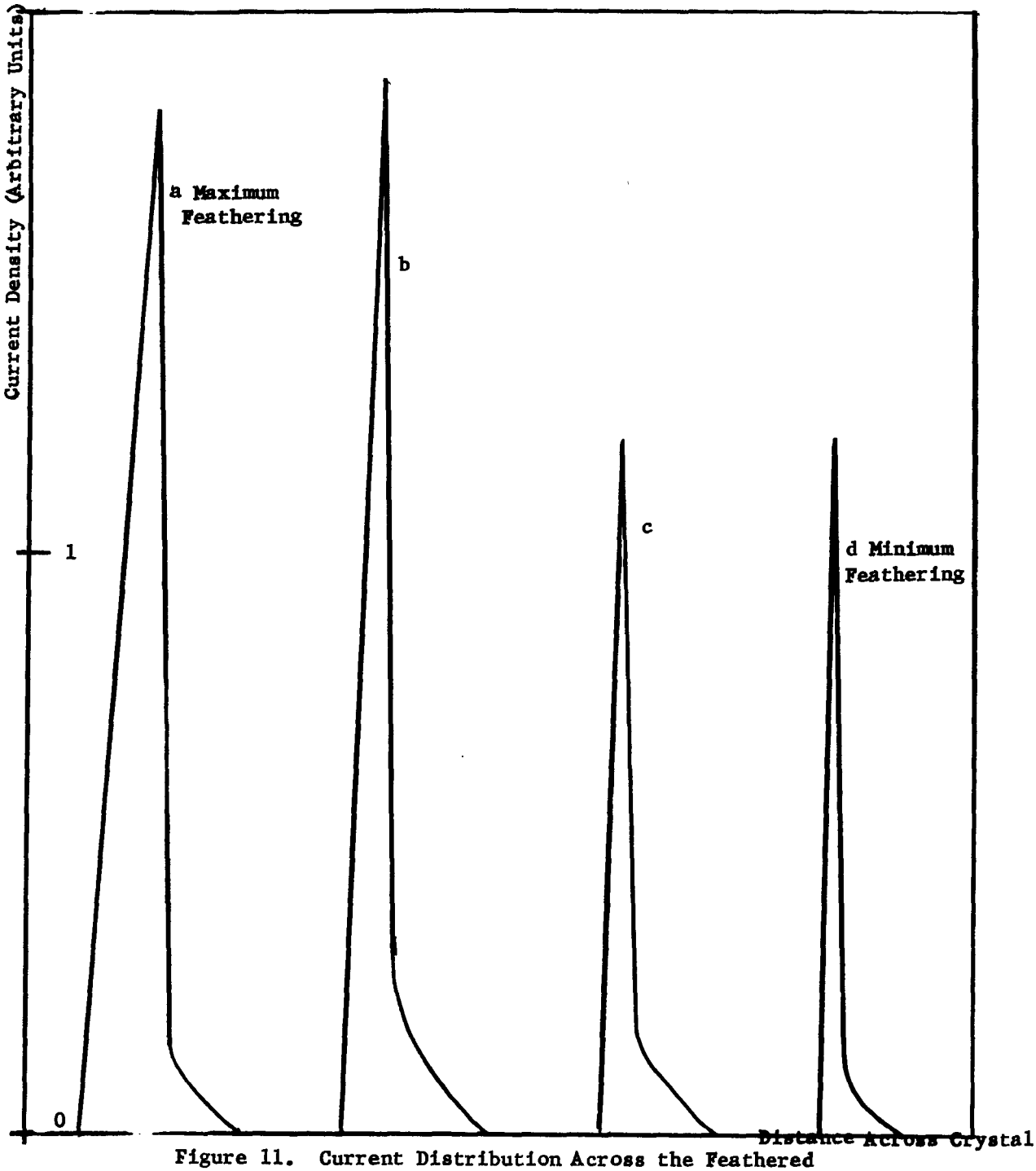

Figure 11. Current Distribution Across the Feathered Edge of Gold at Four Different Positions Along the Edge

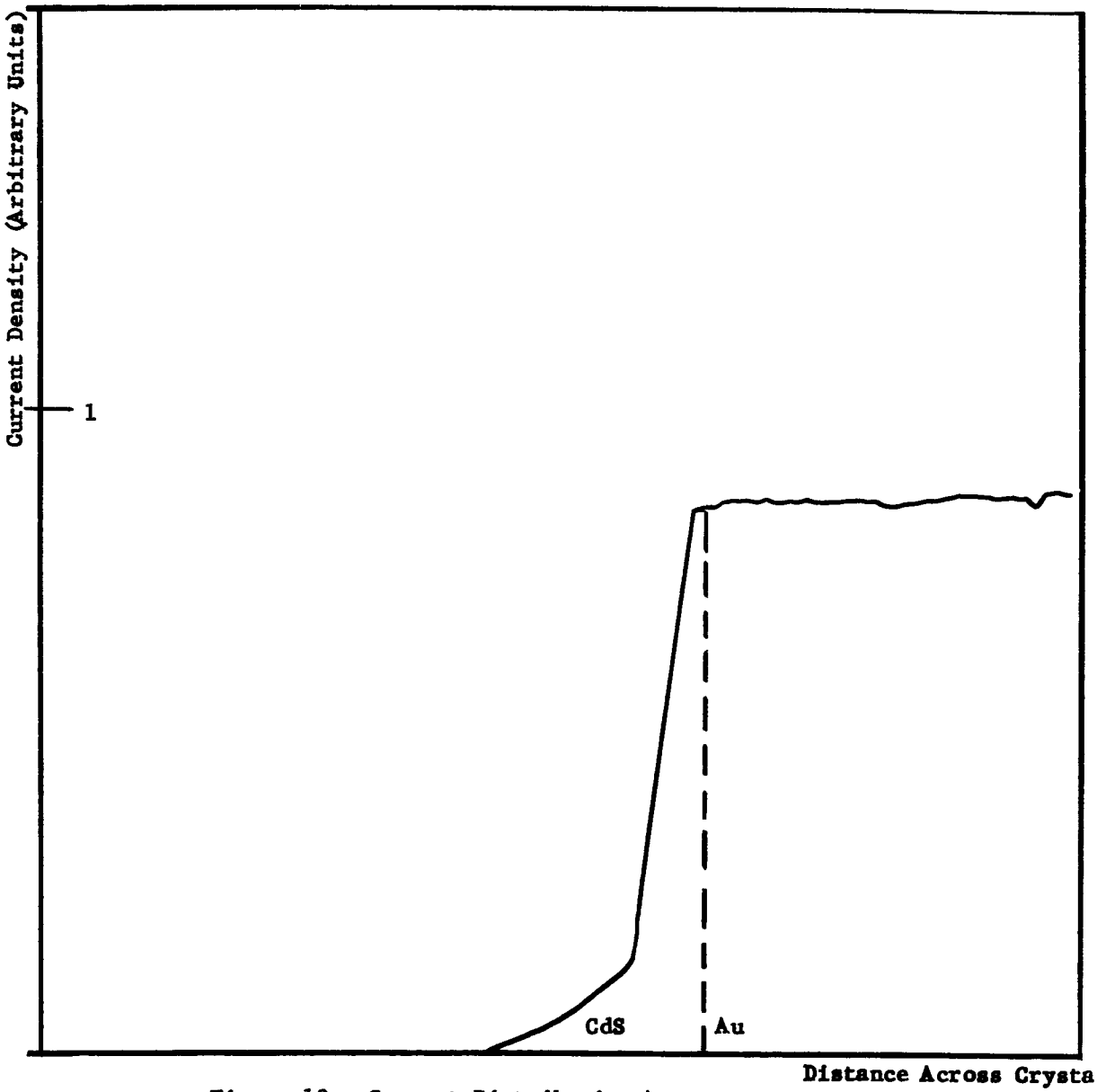

Figure 12. Current Distribution Across Crystal Due to Back-Illumination

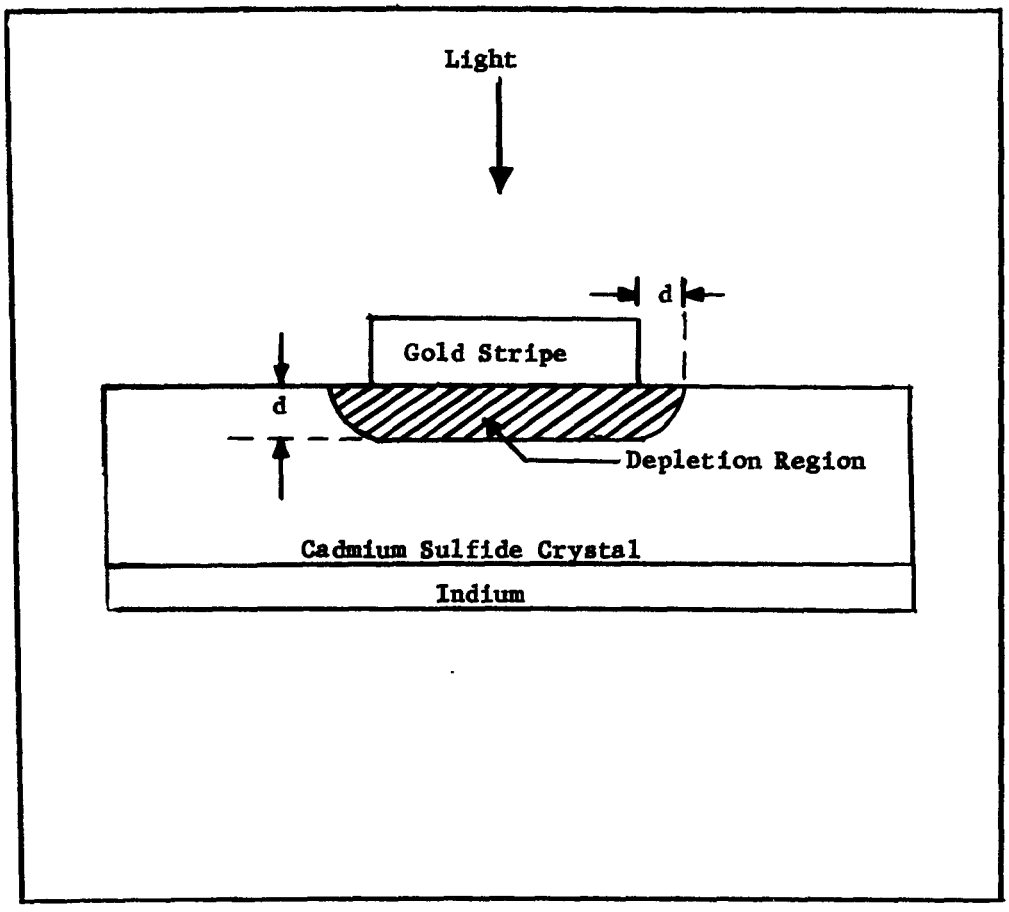

Figure 13. Cross-Section of Gold-Cadmium Sulfide Photocell, Illustrating Depletion Region Geometry

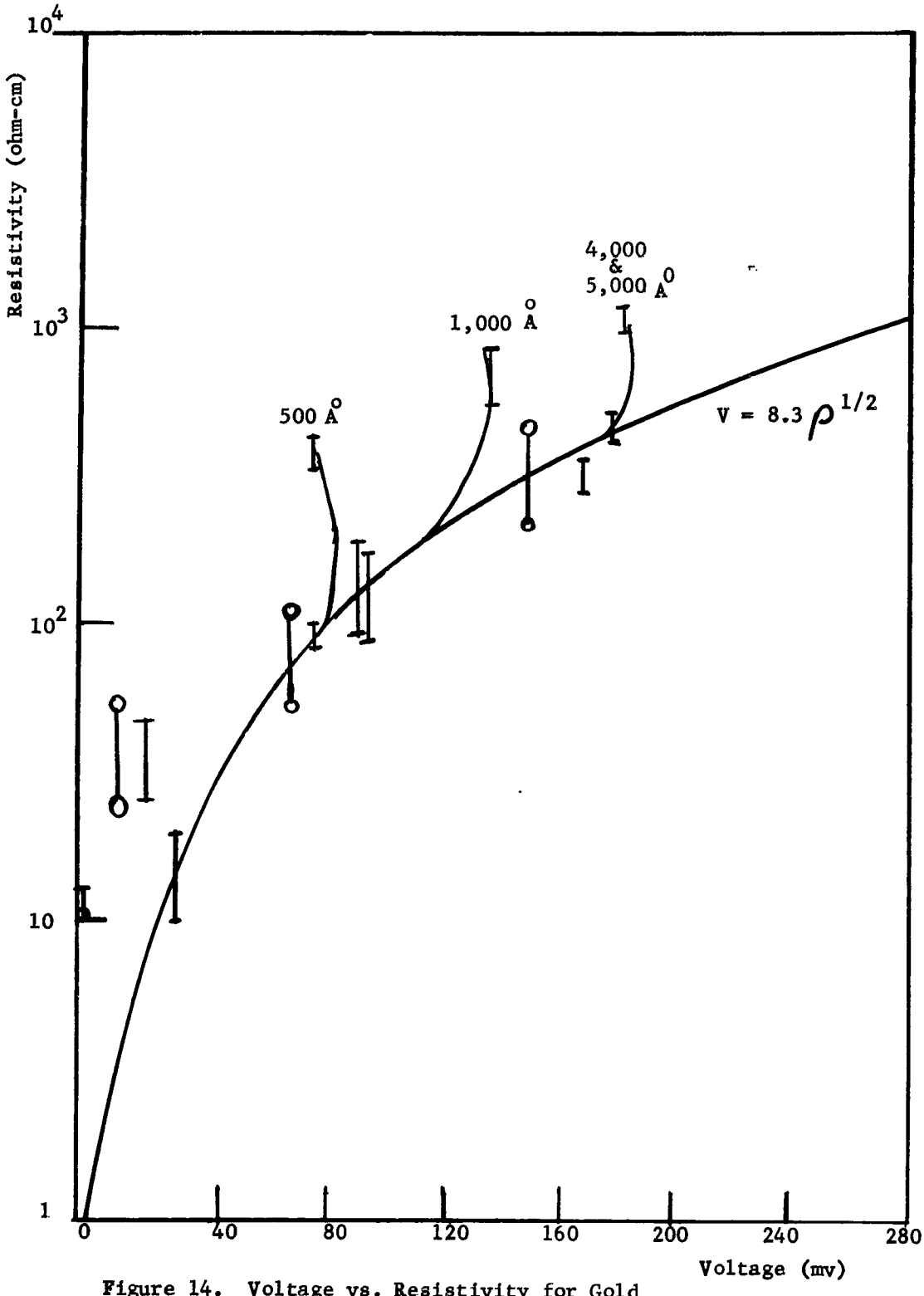

Figure 14. Voltage vs. Resistivity for Gold Films of 500 Å, 1,000 Å, and 4,000 & 5,000 Å at Low Resistivities

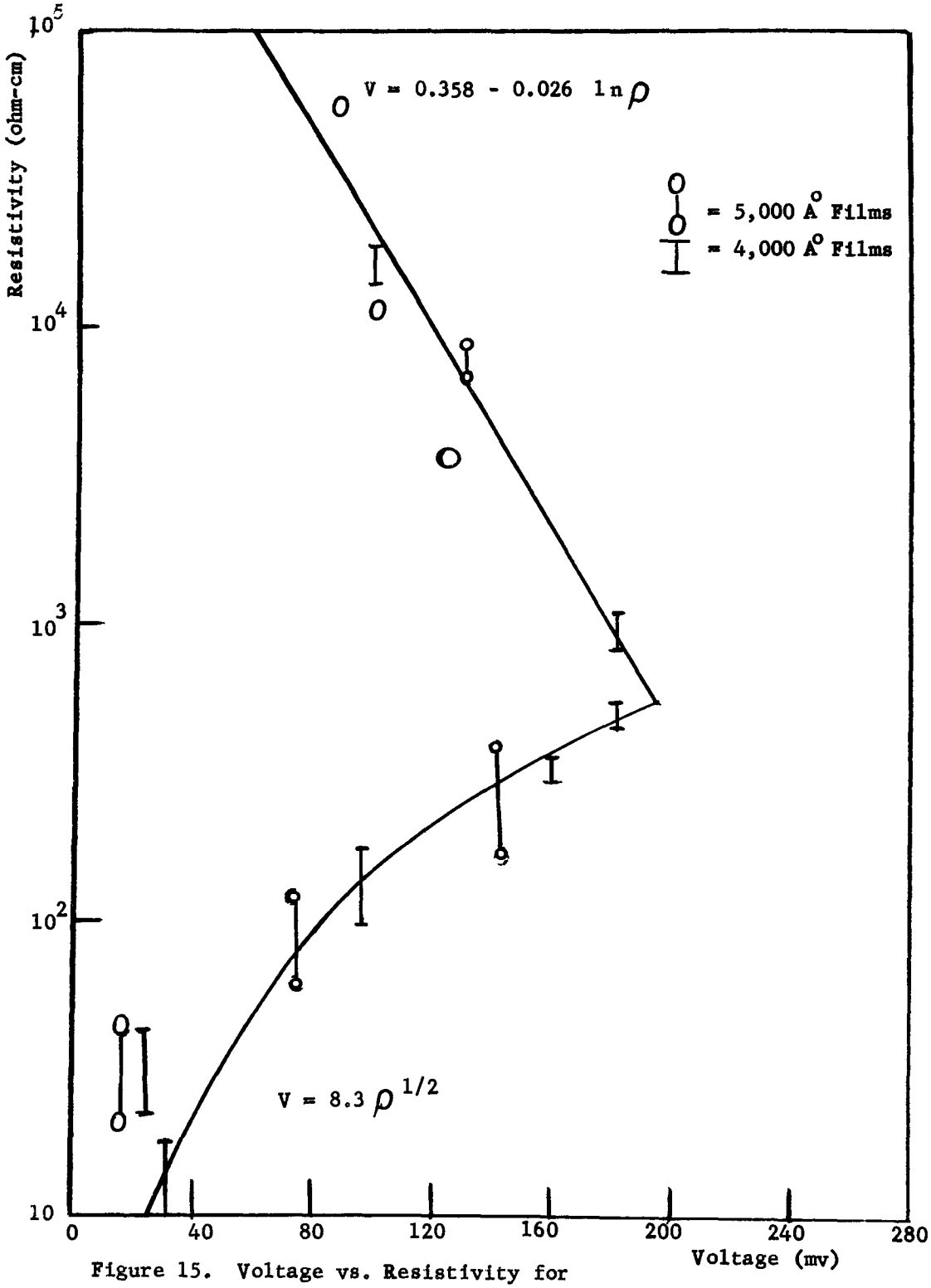

Figure 15. Voltage vs. Resistivity for 4,000 & 5,000 Å Gold Films

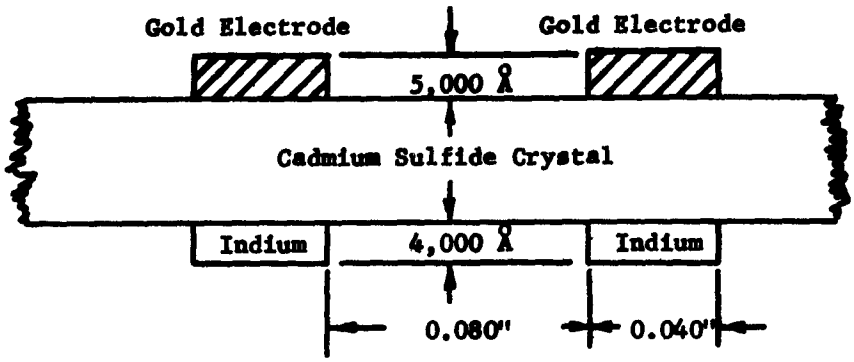

a - Side View of Battery

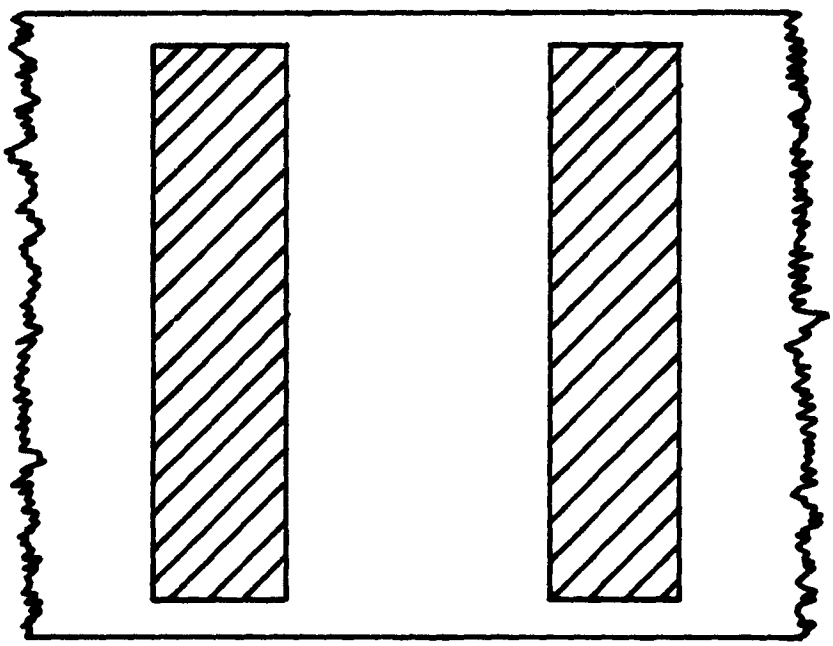

b - Top View of Battery
(Indium stripes under gold stripes)

Figure 16. Cell Design of Batteries Constructed

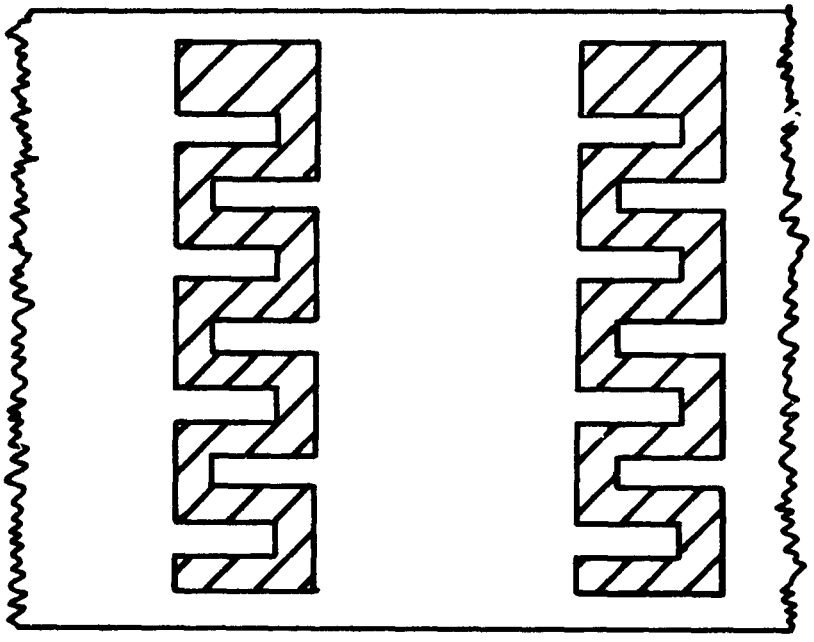

Figure 17. Proposed Geometry of Cathode to Maximize Efficiency of Front-Illuminated Au-CdS Photocell

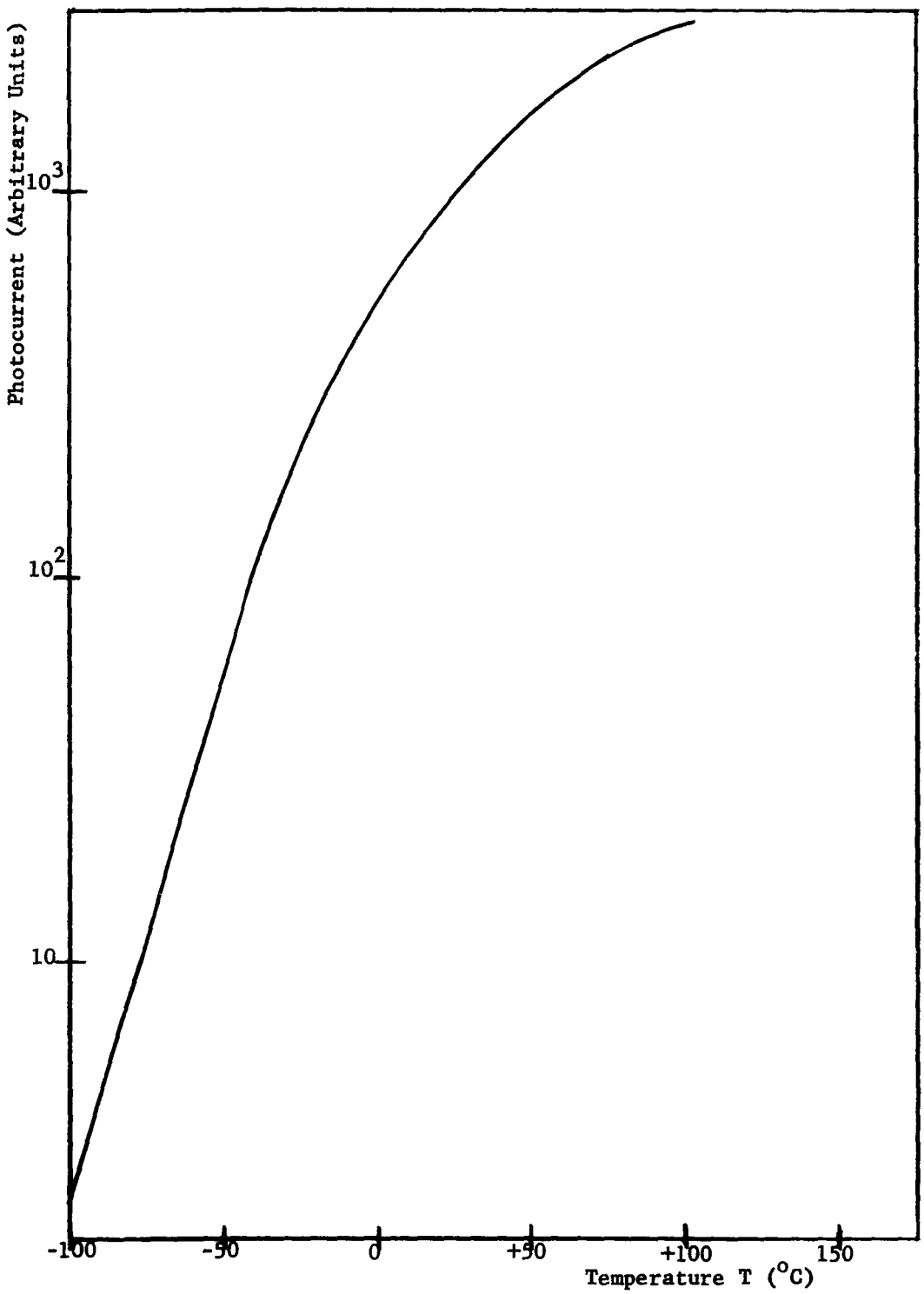

Figure 18. Photovoltaic Current Vs. Temperature

APPENDIX A

PROTOTYPE CELLS

Appendix A contains the data for the three prototype cells.

Construction of Cells:

All three cells were constructed in the following manner:

Etch Treatment: 4% solution of HCL and HNO_3

Bakeout Prior to Gold Evaporation:
2 hours at $125^{o}C$, 5×10^{-5} mm Hg.

Gold Evaporation: 5,000 $\mathring{A}$ thickness
Indium Evaporation: 4,000 $\mathring{A}$ thickness

RESISTIVITY AND PER CENT AREA UTILIZATION
OF CELLS AT 6.3 mw/cm^2

Cell No.	Prior to Bakeout (ohm-cm)	Post Bakeout (ohm-cm)	Per Cent Area Utilization
1	2,000	1,200	0.002
2	600	350	0.001
3	480	280	0.001

CELL EFFICIENCY AT 6.3 mw/cm^2

Cell No.	Per Cent Efficiency (per total area)	Per Cent Effective Efficiency (per utilized area)
1	2.4×10^{-3}	1.2
2	1.3×10^{-3}	1.3
3	4.8×10^{-3}	4.8

TEMPERATURE DEPENDENCE OF CELLS AT 6.3 mw/cm^2

The photovoltage of these cells fluctuates by about 10 percent over the temperature range of -100°C to +100°C.

The photovoltaic current bahaves in an approximately logarithmic manner at low temperatures and appears to saturate above 100°C. A typical graph of photocurrent versus temperature is shown in Fig. 18.

BATTERY 1.

Battery 1.

ILLUMINATION

Cell No.	6.3 mw/cm^2			70 mw/cm^2		
	V_{oc} (mv)		I_{sc} (mμa)	V_{oc} (mv)		I_{sc} (mμa)
	Per Cell	Accumulative	Per Cell	Per Cell	Accumulative	Per Cell
1	110	110	160	110	110	600
2	20	130	360	35	150	1,300
3	20	155	430	35	188	1,600
4	22	175	460	40	226	1,700
5	0	175	10	0	226	200
6	80	250	160	80	305	600
7	40	290	190	40	350	700
8	80	370	200	85	432	700
TOTAL	372	370	200	425	432	850

Cell No.	140 mw/cm^2			420 mw/cm^2		
	V_{oc} (mv)		I_{sc} (mμa)	V_{oc} (mv)		I_{sc} (mμa)
	Per Cell	Accumulative	Per Cell	Per Cell	Accumulative	Per Cell
1	120	120	800	120	120	800
2	40	160	1,500	50	170	1,500
3	40	200	1,800	45	220	1,800
4	45	245	1,900	50	270	1,900
5	0	245	300	0	270	400
6	90	330	800	90	360	800
7	40	370	1,100	45	405	1,100
8	90	460	1,000	90	495	1,000
TOTAL	465	460	1,050	490	495	1,200

TABLE 1. Open-Circuit Voltage and Short-Circuit Current Per Cell, Illumination Levels as Specified.

Battery 1.

Load Resistance (K ohms)	Voltage (mv)	Current (μa)
0	0	200
10	20	190
50	60	185
100	100	180
500	165	160
1,000	200	130
2,000	245	90
3,000	280	52
5,000	300	36
10,000	325	22
20,000	360	12
10^{11}	370	0

TABLE 2. Voltage and Current Vs. Load Resistance at 6.3 mw/cm^2 Illumination.

Load Resistance (K ohms)	Voltage (mv)	Current (μa)
0	0	850
10	25	820
50	72	740
100	110	620
500	170	480
1,000	210	370
2,000	260	240
3,000	300	170
5,000	320	100
10,000	350	46
20,000	400	23
10^{11}	430	0

TABLE 3. Voltage and Current Vs. Load Resistance at 70 mw/cm^2 Illumination.

Battery 1.

Load Resistance (K ohms)	Voltage (mv)	Current (mμa)
0	0	1,050
10	45	1,000
50	97	930
100	150	840
500	210	690
1,000	310	350
2,000	360	190
3,000	400	95
5,000	410	65
10,000	425	36
20,000	440	18
10^{11}	460	0

TABLE 4. Voltage and Current Vs. Load Resistance at 140 mw/cm^2 Illumination.

Load Resistance (K ohms)	Voltage (mv)	Current (mμa)
0	0	1,200
10	50	1,130
50	100	1,100
100	160	1,000
500	275	700
1,000	365	360
2,000	420	190
3,000	455	100
5,000	470	72
10,000	475	46
20,000	480	23
10^{11}	495	0

TABLE 5. Voltage and Current Vs. Load Resistance at 420 mw/cm^2 Illumination.

Battery 1.

Illumination (mw/cm^2)	Voltage V (mv)	Current I (ma)
2.2	300	100
3.5	335	135
4.6	350	160
6.3	370	200
7.2	370	225
8.7	380	260
11.5	385	330
15.4	400	430
21.0	410	500
33.5	420	640
70.	430	850
140.	460	1,050
420.	495	1,200

TABLE 6. Open-Circuit Voltage and Short-Circuit Current Vs. Illumination.

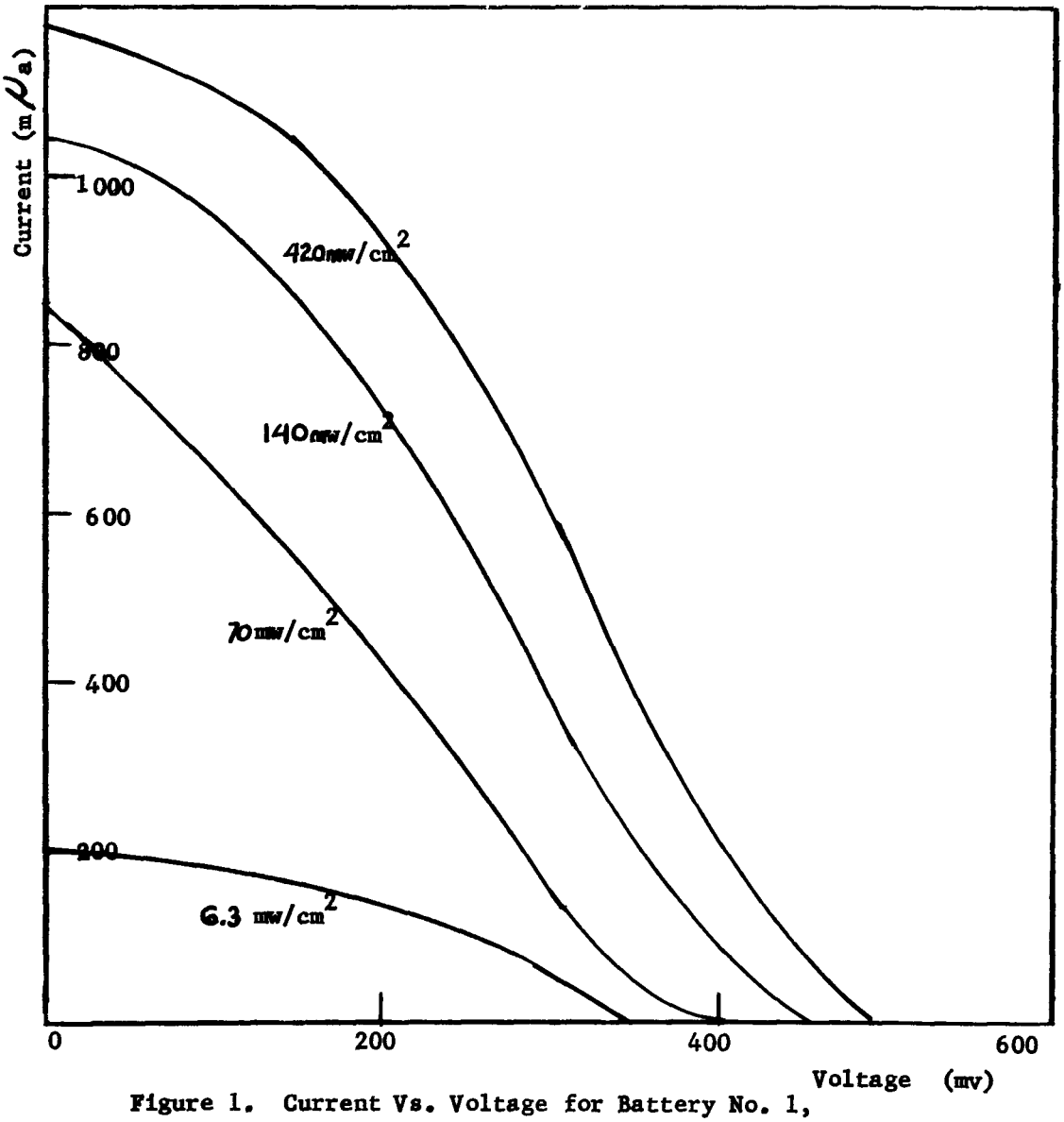

Figure 1. Current Vs. Voltage for Battery No. 1, Illumination Levels as Indicated

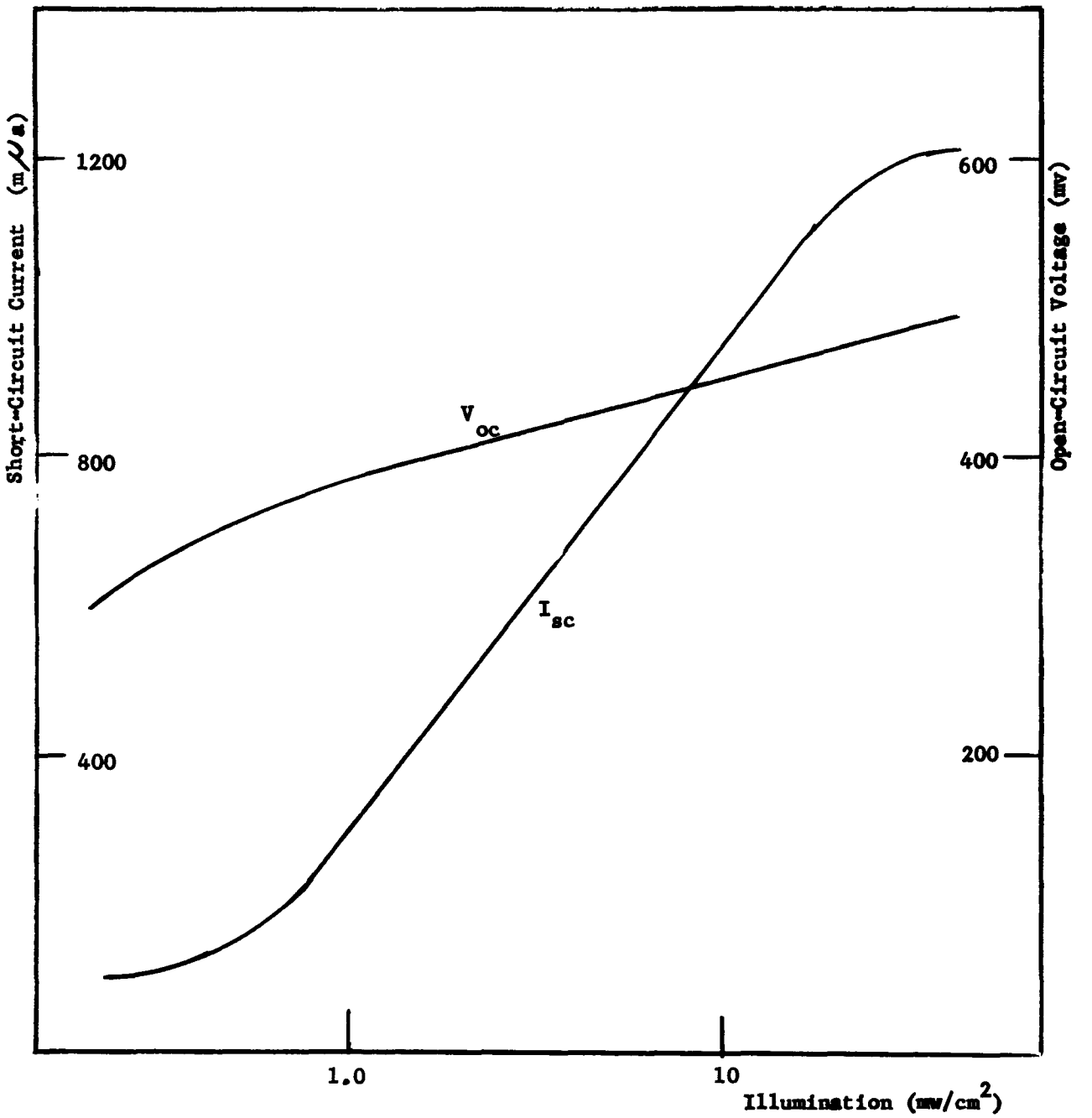

Figure 2. Short-Circuit Current and Open-Circuit Voltage Vs. Illumination for Battery No. 1

BATTERY 2.

Battery 2.

ILLUMINATION

Cell No.	6.3 mw/cm^2			70 mw/cm^2		
	V_{oc} (mv)		I_{sc} (mμa)	V_{oc} (mv)		I_{sc} (mμa)
	Per Cell	Accumulative	Per Cell	Per Cell	Accumulative	Per Cell
1	65	65	110	70	72	120
2	120	185	70	140	210	85
3	120	300	85	145	355	95
4	120	420	35	140	500	50
TOTAL	425	420	60	495	500	85

Cell No.	140 mw/cm^2			420 mw/cm^2		
	V_{oc} (mv)		I_{sc} (mμa)	V_{oc} (mv)		I_{sc} (mμa)
	Per Cell	Accumulative	Per Cell	Per Cell	Accumulative	Per Cell
1	75	75	130	78	80	135
2	150	230	90	155	235	95
3	150	380	95	150	380	102
4	145	525	60	150	530	65
TOTAL	520	525	92	533	530	97

TABLE 1. Open-Circuit Voltage and Short-Circuit Current Per Cell, Illumination Levels as Specified.

Battery 2.

Load Resistance (K ohms)	Voltage (mv)	Current (mμa)
0	0	60
10	40	59
50	100	57
100	160	54
500	210	49
1,000	260	48
2,000	310	36
2,000	340	30
5,000	370	20
10,000	380	12
20,000	400	6
10^{11}	420	0

TABLE 2. Voltage and Current Vs. Load Resistance at 6.3 mw/cm^2 Illumination.

Load Resistance (K ohms)	Voltage (mv)	Current (mμa)
0	0	85
10	58	80
50	116	80
100	180	76
500	240	67
1,000	300	69
2,000	345	63
3,000	450	34
5,000	470	24
10,000	490	16
20,000	490	6
10^{11}	500	0

TABLE 3. Voltage and Current Vs. Load Resistance at 70 mw/cm^2 Illumination.

Battery 2.

Load Resistance (K ohms)	Voltage (mv)	Current (mμa)
0	0	92
10	62	89
50	122	87
100	188	85
500	270	77
1,000	340	71
2,000	360	66
3,000	415	59
5,000	480	26
10,000	500	14
20,000	505	7
10^{11}	525	0

TABLE 4. Voltage and Current Vs. Load Resistance at 140 mw/cm^2 Illumination.

Load Resistance (K ohms)	Voltage (mv)	Current (mμa)
0	0	97
10	71	94
50	130	91
100	200	86
500	280	79
1,000	350	72
2,000	370	69
3,000	435	46
5,000	490	30
10,000	505	15
20,000	512	8
10^{11}	520	0

TABLE 5. Voltage and Current Vs. Load Resistance at 420 mw/cm^2 Illumination.

Battery 2.

Illumination (mw/cm^2)	Voltage V (mv)	Current I (μa)
2.2	330	51
3.5	390	53
4.6	405	56
6.3	420	60
7.2	425	62
8.7	435	64
11.5	440	66
15.4	465	70
21.0	475	73
33.5	485	78
70.	500	85
140.	525	92
420.	530	97

TABLE 6. Open-Circuit Voltage and Short-Circuit Current Vs. Illumination.

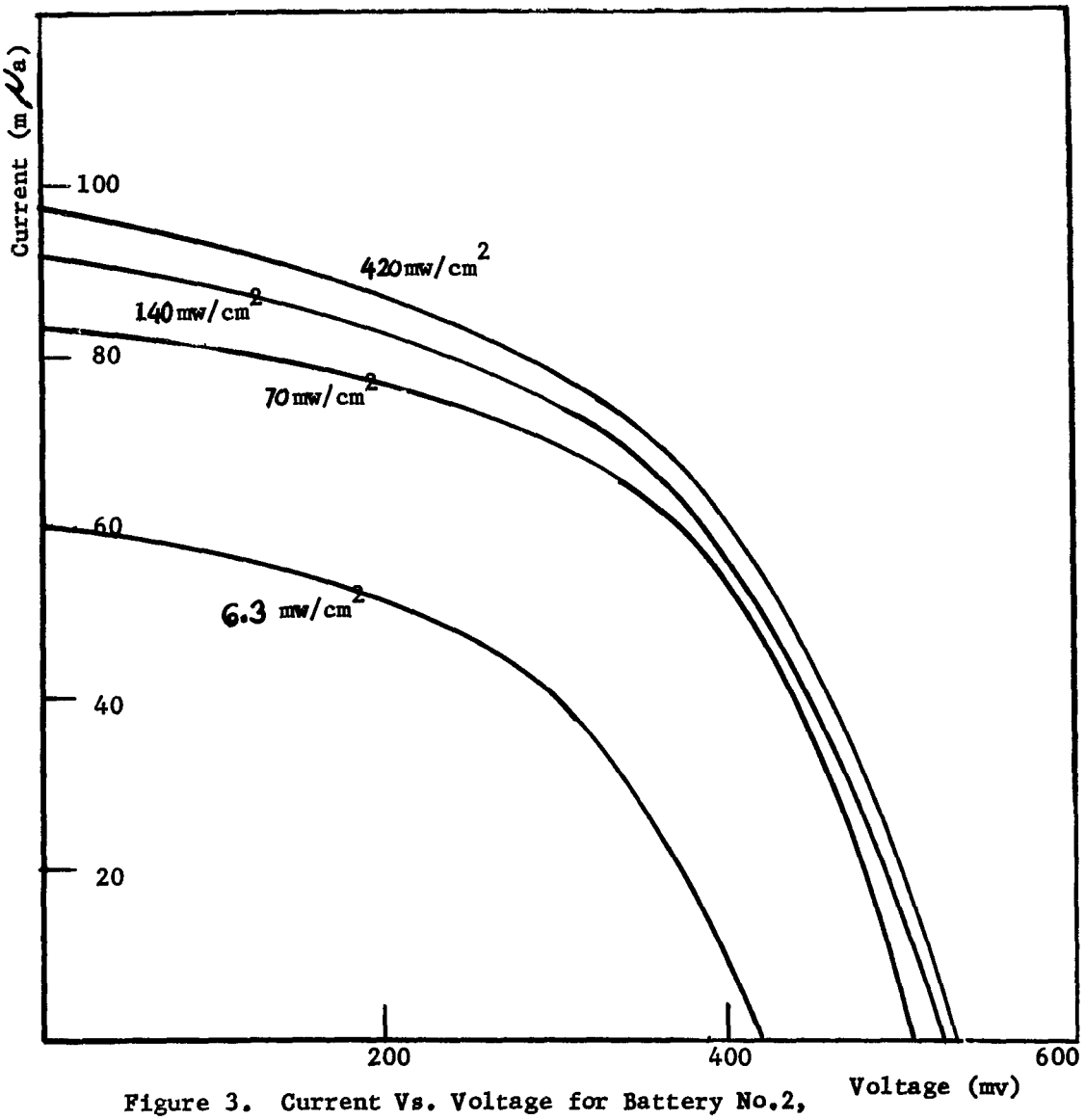

Figure 3. Current Vs. Voltage for Battery No.2, Illumination Levels as Indicated

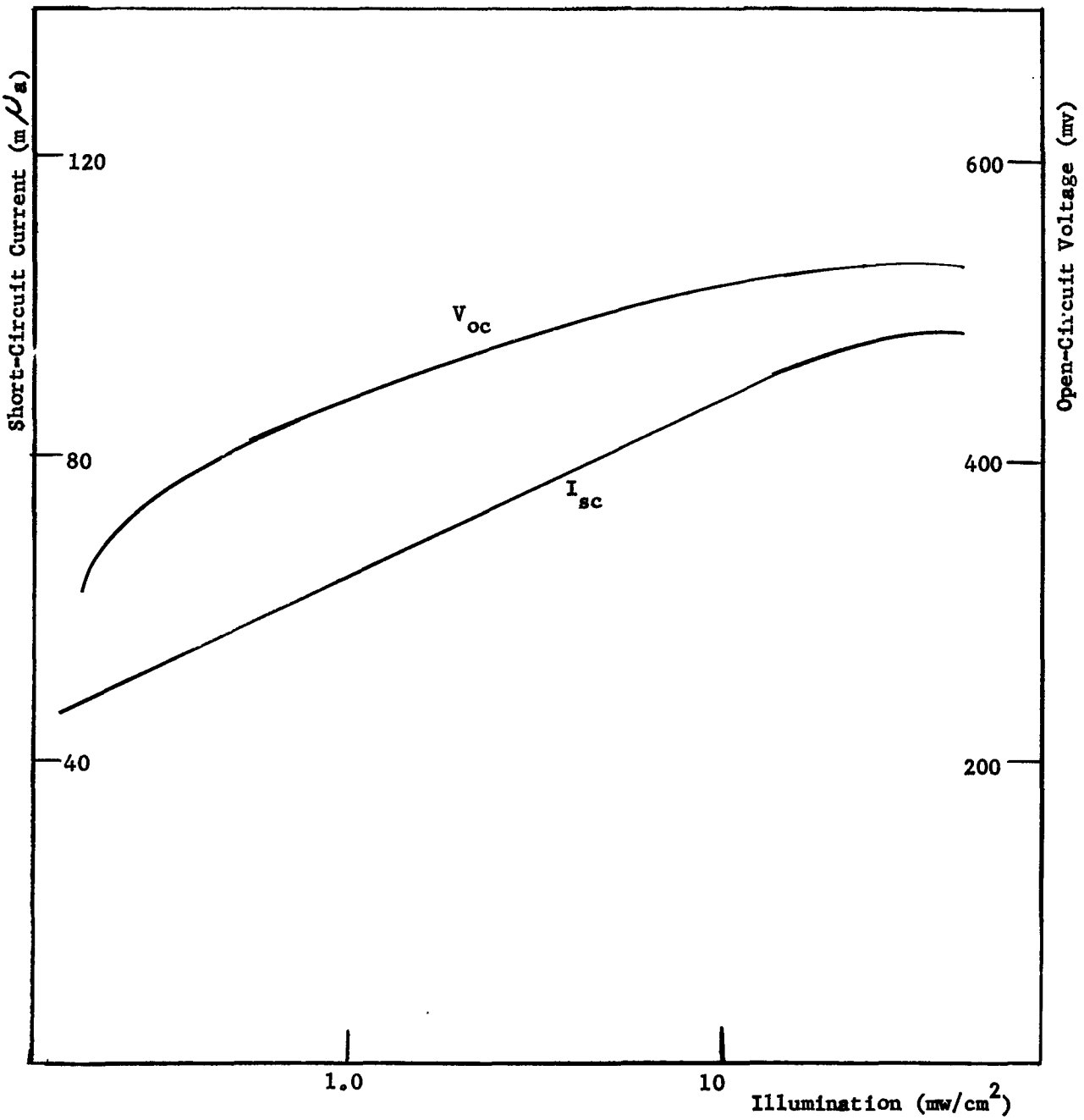

Figure 4. Short-Circuit Current and Open-Circuit Voltage Vs. Illumination for Battery No. 2

BATTERY 3.

Battery 3.

ILLUMINATION

Cell No.	6.3 mw/cm^2			70 mw/cm^2		
	V_{oc} (mv)		I_{sc} (mμa)	V_{oc} (mv)		I_{sc} (mμa)
	Per Cell	Accumulative	Per Cell	Per Cell	Accumulative	Per Cell
1	200	200	300	220	200	1,400
2	140	330	200	200	410	1,100
3	60	390	105	60	475	520
4 (damaged in construction)						
TOTAL	400	390	240	480	475	1,050

Cell No.	140 mw/cm^2			420 mw/cm^2		
	V_{oc} (mv)		I_{sc} (mμa)	V_{oc} (mv)		I_{sc} (mμa)
	Per Cell	Accumulative	Per Cell	Per Cell	Accumulative	Per Cell
1	250	240	2,300	250	250	3,100
2	280	515	2,200	310	560	2,900
3	90	610	950	85	650	1,450
4 (damaged in construction)						
TOTAL	620	610	2,000	645	650	2,800

TABLE 1. Open-Circuit Voltage and Short-Circuit Current Per Cell, Illumination Levels as Specified.

Battery 3.

Load Resistance (K ohms)	Voltage (mv)	Current (m μ a)
0	0	240
10	2	220
50	11	220
100	21	215
500	90	195
1,000	160	170
2,000	240	130
3,000	280	110
5,000	330	74
10,000	370	42
20,000	400	22
10^{11}	430	0

TABLE 2. Voltage and Current Vs. Load Resistance at 6.3 mw/cm^2 Illumination.

Load Resistance (K ohms)	Voltage (mv)	Current (m μ a)
0	0	1,050
10	20	940
50	50	880
100	80	820
500	260	570
1,000	320	400
2,000	370	240
3,000	390	160
5,000	410	100
10,000	420	50
20,000	440	30
10^{11}	475	0

TABLE 3. Voltage and Current Vs. Load Resistance at 70 mw/cm^2 Illumination.

Battery 3.

Load Resistance (K ohms)	Voltage (mv)	Current (mμa)
0	0	2,000
10	30	1,950
50	70	1,850
100	110	1,760
500	290	1,260
1,000	360	1,000
2,000	410	690
3,000	450	410
5,000	480	330
10,000	510	210
20,000	570	50
10^{11}	610	0

TABLE 4. Voltage and Current Vs. Load Resistance at 140 mw/cm^2 Illumination.

Load Resistance (K ohms)	Voltage (mv)	Current (mμa)
0	0	2,800
10	35	2,700
50	80	2,550
100	115	2,450
500	300	1,700
1,000	380	1,200
2,000	425	850
3,000	465	620
5,000	500	430
10,000	520	330
20,000	580	110
10^{11}	645	0

TABLE 5. Voltage and Current Vs. Load Resistance at 420 mw/cm^2 Illumination.

Battery 3.

Illumination (mw/cm^2)	Voltage V (mv)	Current I (mμa)
2.2	340	70
3.5	380	98
4.6	400	125
6.3	410	200
7.2	430	215
8.7	440	265
11.5	460	300
15.4	480	400
21.0	500	520
33.5	530	730
70.	580	1,050
140.	610	2,000
420.	645	2,800

TABLE 6. Open-Circuit Voltage and Short-Circuit Current Vs. Illumination.

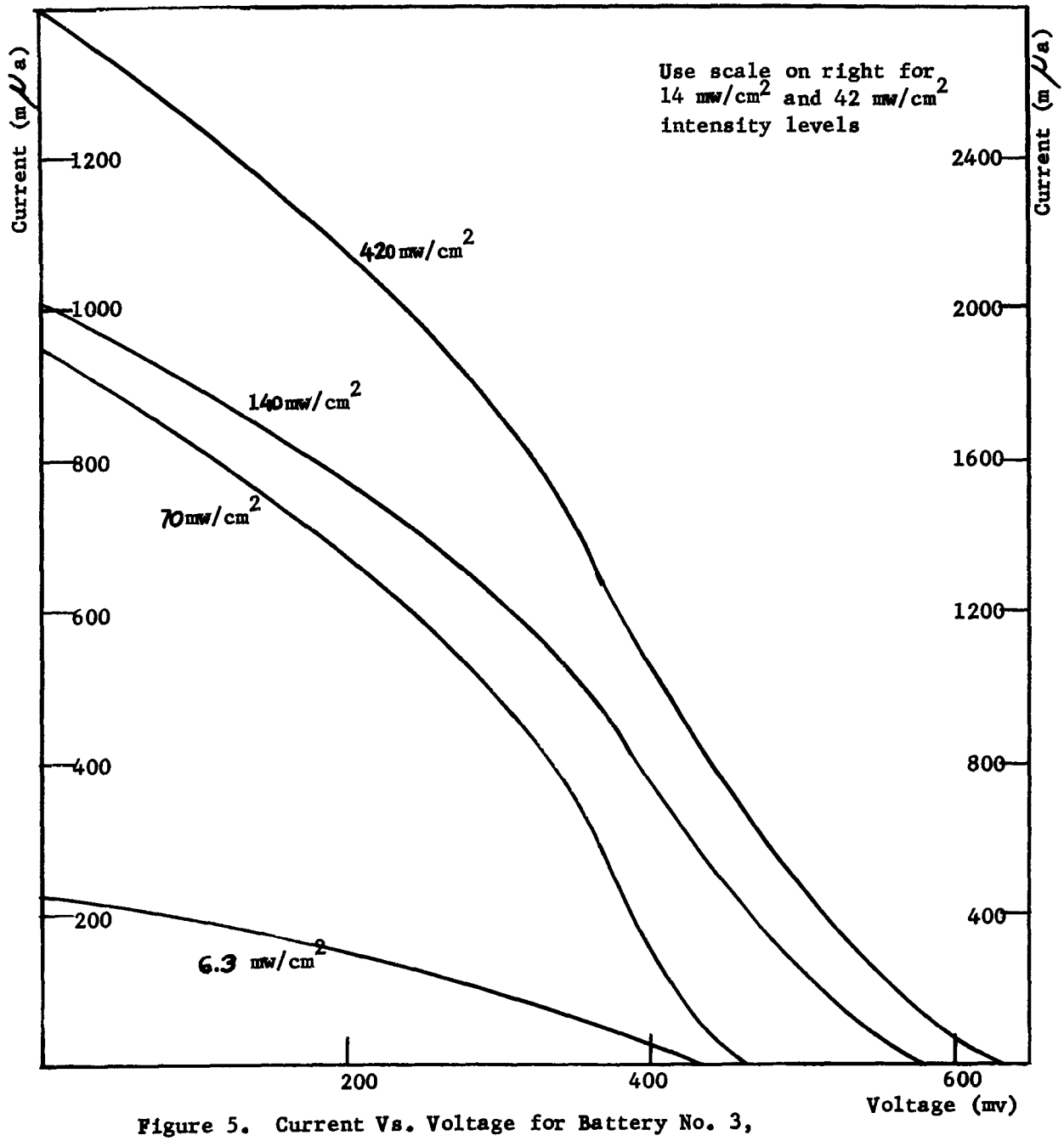

Figure 5. Current Vs. Voltage for Battery No. 3, Illumination Levels as Indicated

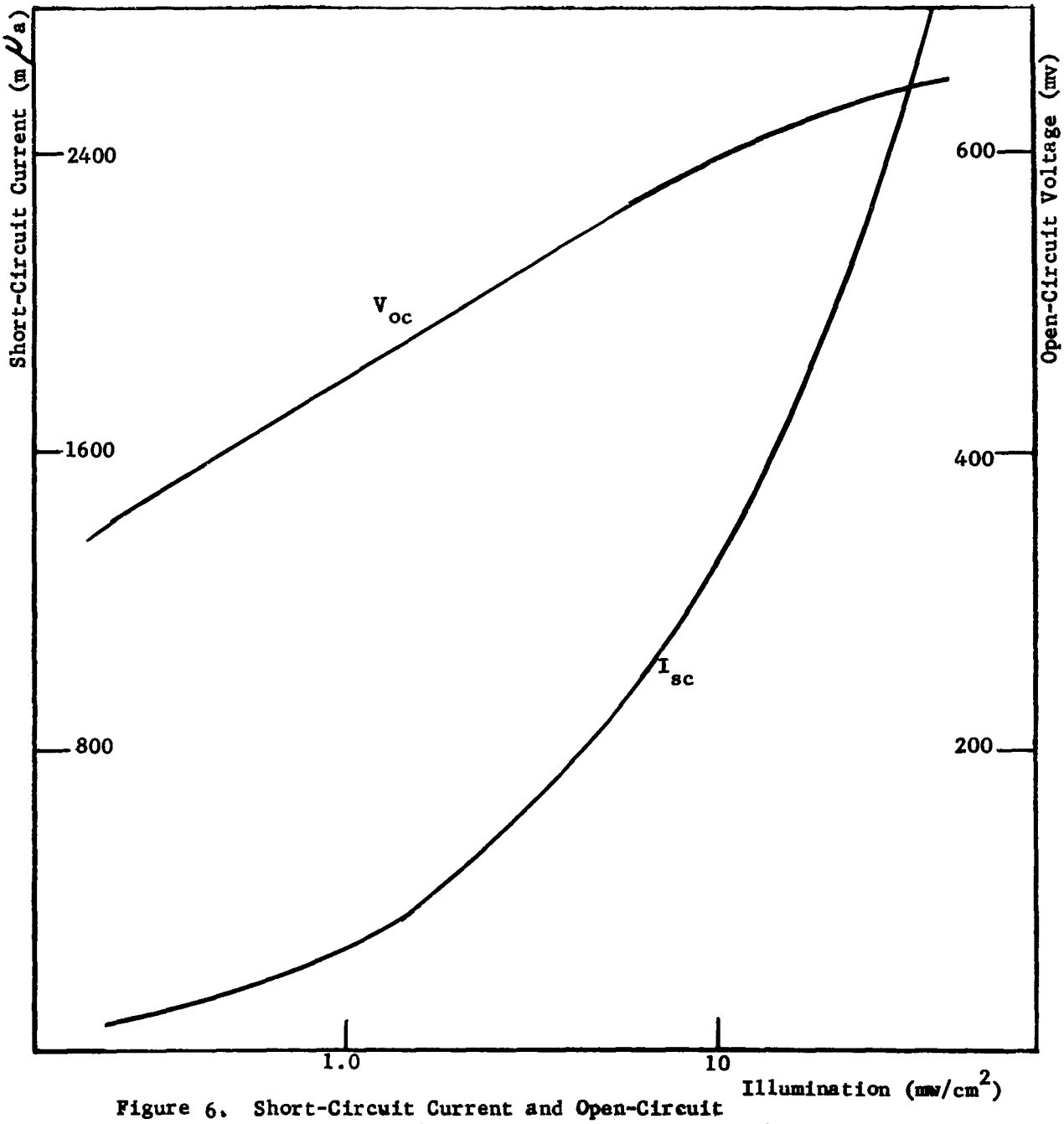

Figure 6. Short-Circuit Current and Open-Circuit Voltage Vs. Illumination for Battery No. 3